

ROBIN SCHWARZ ALGORITHM FOR THE NICEM METHOD: THE P_Q FINITE ELEMENT CASE

CAROLINE JAPHET*, YVON MADAY†, AND FRÉDÉRIC NATAF‡

Abstract. In [16, 25] we proposed a new non-conforming domain decomposition paradigm, the New Interface Cement Equilibrated Mortar (NICEM) method, based on Schwarz type methods that allows for the use of Robin interface conditions on non-conforming grids. The error analysis was done for P_1 finite elements, in 2D and 3D. In this paper, we provide new numerical analysis results that allow to extend this error analysis in 2D for piecewise polynomials of higher order and also prove the convergence of the iterative algorithm in all these cases.

Key words. Optimized Schwarz domain decomposition, Robin transmission conditions, finite element methods, non-conforming grids, error analysis, piecewise polynomials of high order, NICEM method.

1. Introduction. The New Interface Cement Equilibrated Mortar (NICEM) method proposed in [16] is an equilibrated mortar domain decomposition method that allows for the use of optimized Schwarz algorithms with Robin interface conditions on non-conforming grids. It has been analyzed in [25] in 2D and 3D for P_1 elements.

The purpose of this paper is to extend this numerical analysis in 2D for piecewise polynomials of higher order. We thus establish new numerical analysis results in the frame of finite element approximation and also present the iterative algorithm and prove its convergence in all these cases.

We first consider the problem at the continuous level: Find u such that

$$\mathcal{L}(u) = f \text{ in } \Omega \quad (1.1)$$

$$\mathcal{C}(u) = g \text{ on } \partial\Omega \quad (1.2)$$

where \mathcal{L} and \mathcal{C} are partial differential equations. The original Schwarz algorithm is based on a decomposition of the domain Ω into overlapping subdomains and the resolution of Dirichlet boundary value problems in each subdomain. It has been proposed in [30] to use more general interface/boundary conditions for the problems on the subdomains in order to use a non-overlapping decomposition of the domain. The convergence factor is also dramatically reduced. More precisely, let Ω be a $\mathcal{C}^{1,1}$ (or convex polygon in 2D or polyhedron in 3D) domain of \mathbb{R}^d , $d = 2$ or 3 ; we assume it is decomposed into K non-overlapping subdomains: $\overline{\Omega} = \cup_{k=1}^K \overline{\Omega}^k$. We suppose that the subdomains Ω^k , $1 \leq k \leq K$ are either $\mathcal{C}^{1,1}$ or polygons in 2D or polyhedrons in 3D. We assume also that this decomposition is geometrically conforming in the sense that the intersection of the closure of two different subdomains, if not empty, is either a common vertex, a common edge, or a common face of the subdomains in 3D¹. Let

*Université Paris 13, Sorbonne Paris Cité, LAGA, CNRS UMR 7539, 99 Avenue J-B Clément, F-93430 Villetaneuse, France; INRIA Paris-Rocquencourt, BP 105, 78153 Le Chesnay, France; CSCAMM, University of Maryland College Park, MD 20742 USA, E-mail: japhet@math.univ-paris13.fr; Partially supported by GNR MoMaS.

†UPMC Univ Paris 06, UMR 7598, Laboratoire Jacques-Louis Lions, F-75005, Paris, France; Institut Universitaire de France; and Brown Univ, Division of Applied Maths, Providence, RI, USA, E-mail: maday@ann.jussieu.fr.

‡CNRS, UMR 7598, Laboratoire Jacques-Louis Lions, F-75005, Paris, France; UPMC Univ Paris 06, UMR 7598, Laboratoire Jacques-Louis Lions, F-75005, Paris, France, E-mail: nataf@ann.jussieu.fr.

¹This assumption is not restrictive since in the case of a partition geometrically non-conforming, the faces can be decomposed in subfaces to obtain a geometrical conformity

\mathbf{n}_k be the outward normal from Ω^k . Let $(\mathcal{B}_{k,\ell})_{1 \leq k, \ell \leq K, k \neq \ell}$ be the chosen transmission conditions on the interface between subdomains Ω^k and Ω^ℓ (e.g. $\mathcal{B}_{k,\ell} = \frac{\partial}{\partial \mathbf{n}_k} + \alpha_k$). What we shall call here a Schwarz type method for the problem (1.1)-(1.2) is its reformulation: Find $(u_k)_{1 \leq k \leq K}$ such that

$$\begin{aligned}\mathcal{L}(u_k) &= f \text{ in } \Omega^k \\ \mathcal{C}(u_k) &= g \text{ on } \partial\Omega^k \cap \partial\Omega \\ \mathcal{B}_{k,\ell}(u_k) &= \mathcal{B}_{k,\ell}(u_\ell) \text{ on } \partial\Omega^k \cap \partial\Omega^\ell,\end{aligned}$$

leading to the iterative procedure

$$\begin{aligned}\mathcal{L}(u_k^{n+1}) &= f \text{ in } \Omega^k \\ \mathcal{C}(u_k^{n+1}) &= g \text{ on } \partial\Omega^k \cap \partial\Omega \\ \mathcal{B}_{k,\ell}(u_k^{n+1}) &= \mathcal{B}_{k,\ell}(u_\ell^n) \text{ on } \partial\Omega^k \cap \partial\Omega^\ell.\end{aligned}$$

The convergence factor of associated Schwarz-type domain decomposition methods depends largely on the choice of the transmission operators $\mathcal{B}_{k,\ell}$ (see for instance [20, 33, 19, 18, 13, 14, 29, 4, 38, 31, 10] and [32, 17]). More precisely, transmission conditions which reduce dramatically the convergence factor of the algorithm have been proposed (see [23, 22, 24]) for a convection-diffusion equation, where coefficients in second order transmission conditions were optimized.

On the other hand, the mortar element method, first introduced in [8], enables the use of non-conforming grids, and thus parallel generation of meshes, local adaptive meshes and fast and independent solvers. It is also well suited to the use of "Dirichlet-Neumann" ([17]), or "Neumann-Neumann" preconditioned conjugate gradient method applied to the Schur complement matrix [27, 2, 36]. In [1], a new cement to match Robin interface conditions with non-conforming grids in the case of a finite volume discretization was introduced and analyzed. Such an approach has been extended to a finite element discretization in [16]. A variant has been independently implemented in [28] for the Maxwell equations, without numerical analysis. Another approach, in the finite volume case, has been proposed in [35].

The numerical analysis of the NICEM method proposed in [16] is done in [25] for \mathbf{P}_1 finite elements, in 2D and 3D. These results are for interface conditions of order 0 (i.e. $\mathcal{B}_{k,\ell} = \frac{\partial}{\partial \mathbf{n}_k} + \alpha_k$) and are the prerequisites for the goal in designing this non-overlapping method for interface conditions such as Ventcel interface conditions which greatly enhance the information exchange between subdomains, see [26] for preliminary results on the extension of the NICEM method to Ventcel conditions.

The purpose of this paper is first to present a general finite element NICEM method in the case of \mathbf{P}_p finite elements, with $p \geq 1$ in 2D and $p = 1$ in 3D. We also provide a Robin iterative algorithm and prove its convergence. Then, we present in full details the error analysis in the case of piecewise polynomials of high order in 2D.

In Section 2, we describe the NICEM method in 2D and 3D. Then, in Section 3, we present the iterative algorithm at the continuous and discrete levels, and we prove, in both cases, the well-posedness and convergence of the iterative method, for polynomials of low and high order in 2D, and for \mathbf{P}_1 finite elements in 3D. The convergence is also proven in 3D for \mathbf{P}_p finite elements, $p \geq 1$, in a weak sense. In Section 4 we extend the error estimates analysis given in [25] to 2D piecewise polynomials of higher order. We finally present in Section 5 simulations for two and four subdomains, that fit the theoretical estimates.

2. Definition of the method. We consider the following problem : Find u such that

$$(Id - \Delta)u = f \quad \text{in } \Omega \quad (2.1)$$

$$u = 0 \quad \text{on } \partial\Omega, \quad (2.2)$$

where f is given in $L^2(\Omega)$.

The variational statement of the problem (2.1)-(2.2) consists in writing the problem as follows : Find $u \in H_0^1(\Omega)$ such that

$$\int_{\Omega} (\nabla u \nabla v + uv) dx = \int_{\Omega} f v dx, \quad \forall v \in H_0^1(\Omega). \quad (2.3)$$

We introduce the space $H_*^1(\Omega^k)$ defined by

$$H_*^1(\Omega^k) = \{\varphi \in H^1(\Omega^k), \quad \varphi = 0 \text{ over } \partial\Omega \cap \partial\Omega^k\},$$

and we introduce $\Gamma^{k,\ell}$ the interface of two adjacent subdomains, $\Gamma^{k,\ell} = \partial\Omega^k \cap \partial\Omega^\ell$.

It is standard to note that the space $H_0^1(\Omega)$ can then be identified with the subspace of the K -tuple $\underline{v} = (v_1, \dots, v_K)$ that are continuous on the interfaces:

$$V = \{\underline{v} = (v_1, \dots, v_K) \in \prod_{k=1}^K H_*^1(\Omega^k), \quad \forall k, \ell, k \neq \ell, \quad 1 \leq k, \ell \leq K, \quad v_k = v_\ell \text{ over } \Gamma^{k,\ell}\}.$$

Following [25], in order to glue non-conforming grids with Robin transmission conditions, we impose the constraint $v_k = v_\ell$ over $\Gamma^{k,\ell}$ through a Lagrange multiplier in $H^{-1/2}(\partial\Omega^k)$. The constrained space is then defined as follows

$$\mathcal{V} = \{(\underline{v}, \underline{q}) \in \left(\prod_{k=1}^K H_*^1(\Omega^k) \right) \times \left(\prod_{k=1}^K H^{-1/2}(\partial\Omega^k) \right), \\ v_k = v_\ell \text{ and } q_k = -q_\ell \text{ over } \Gamma^{k,\ell}, \quad \forall k, \ell\}. \quad (2.4)$$

Then, problem (2.3) is equivalent to the following one (see [25]): Find $(\underline{u}, \underline{p}) \in \mathcal{V}$ such that

$$\sum_{k=1}^K \int_{\Omega^k} (\nabla u_k \nabla v_k + u_k v_k) dx - \sum_{k=1}^K \int_{\partial\Omega^k} p_k v_k = \int_{\Omega} f v dx, \quad \forall \underline{v} \in \prod_{k=1}^K H_*^1(\Omega^k).$$

Being equivalent with the original problem, where $p_k = \frac{\partial u}{\partial \mathbf{n}_k}$ over $\partial\Omega^k$, this problem is well posed. This can also be directly derived from the proof of an inf-sup condition that follows from the arguments developed hereafter for the analysis of the iterative procedure.

Note that the Dirichlet-Neumann condition in (2.4) is equivalent to the following combined equality

$$p_k + \alpha u_k = -p_\ell + \alpha u_\ell \quad \text{over } \Gamma^{k,\ell}, \quad \forall k, \ell. \quad (2.5)$$

As noticed in [25], for regular enough function it is also equivalent to

$$\int_{\Gamma^{k,\ell}} ((p_k + \alpha u_k) - (-p_\ell + \alpha u_\ell)) \psi_{k,\ell} = 0, \quad \forall \psi_{k,\ell} \in L^2(\Gamma^{k,\ell}), \quad \forall k, \ell, \quad (2.6)$$

which is the form under which the discrete method is described.

Let us describe the method in the non-conforming discrete case.

2.1. Discrete case. We introduce now the discrete spaces for piecewise polynomials of higher order in 2D. Each Ω^k is provided with its own mesh \mathcal{T}_h^k , $1 \leq k \leq K$, such that

$$\bar{\Omega}^k = \cup_{T \in \mathcal{T}_h^k} T.$$

For $T \in \mathcal{T}_h^k$, let h_T be the diameter of T ($h_T = \sup_{x,y \in T} d(x,y)$) and h the discretization parameter $h = \max_{1 \leq k \leq K} h_k$, with $h_k = \max_{T \in \mathcal{T}_h^k} h_T$. As noticed in [25], for the sake of readability we prefer to use h instead of h_k , but all the analysis could be performed with h_k instead of h . Let ρ_T be the diameter of the circle (in 2D) or sphere (in 3D) inscribed in T , then $\sigma_T = \frac{h_T}{\rho_T}$ is a measure of the non-degeneracy of T . We suppose that \mathcal{T}_h^k is uniformly regular: there exists σ and τ independent of h such that $\forall T \in \mathcal{T}_h^k$, $\sigma_T \leq \sigma$, $\tau h \leq h_T$. We consider that the sets belonging to the meshes are of simplicial type (triangles), but the analysis made hereafter can be applied as well for quadrangular meshes. Let $\mathbf{P}_p(T)$ denote the space of all polynomials defined over T of total degree less than or equal to p . The finite elements are of Lagrangian type, of class \mathcal{C}^0 . We define over each subdomain two conforming spaces Y_h^k and X_h^k by:

$$\begin{aligned} Y_h^k &= \{v_{h,k} \in \mathcal{C}^0(\bar{\Omega}^k), v_{h,k}|_T \in \mathbf{P}_p(T), \forall T \in \mathcal{T}_h^k\}, \\ X_h^k &= \{v_{h,k} \in Y_h^k, v_{h,k}|_{\partial\Omega^k \cap \partial\Omega} = 0\}. \end{aligned}$$

In what follows we assume that the mesh is designed by taking into account the geometry of the $\Gamma^{k,\ell}$ in the sense that, the space of traces over each $\Gamma^{k,\ell}$ of elements of Y_h^k is a finite element space denoted by $\mathcal{Y}_h^{k,\ell}$. Let k be given, the space \mathcal{Y}_h^k is then the product space of the $\mathcal{Y}_h^{k,\ell}$ over each ℓ such that $\Gamma^{k,\ell} \neq \emptyset$. With each such interface we associate a subspace $\tilde{W}_h^{k,\ell}$ of $\mathcal{Y}_h^{k,\ell}$ in the same spirit as in the mortar element method [8] in 2D or [6] and [9] in 3D. To be more specific, in 2D if the space X_h^k consists of continuous piecewise polynomials of degree $\leq p$, then it is readily noticed that the restriction of X_h^k to $\Gamma^{k,\ell}$ consists in finite element functions adapted to the (possibly curved) side $\Gamma^{k,\ell}$ of piecewise polynomials of degree $\leq p$. This side has two end points that we denote as $x_0^{k,\ell}$ and $x_N^{k,\ell}$ that belong to the set of vertices of the corresponding triangulation of $\Gamma^{k,\ell}$: $x_0^{k,\ell}, x_1^{k,\ell}, \dots, x_{N-1}^{k,\ell}, x_N^{k,\ell}$. The space $\tilde{W}_h^{k,\ell}$ is then the subspace of those elements of $\mathcal{Y}_h^{k,\ell}$ that are polynomials of degree $\leq p-1$ over both $[x_0^{k,\ell}, x_1^{k,\ell}]$ and $[x_{N-1}^{k,\ell}, x_N^{k,\ell}]$. As before, the space \tilde{W}_h^k is the product space of the $\tilde{W}_h^{k,\ell}$ over each ℓ such that $\Gamma^{k,\ell} \neq \emptyset$. Let α be a given positive real number. Following [25], the discrete constrained space is defined as

$$\begin{aligned} \mathcal{V}_h &= \{(\underline{u}_h, \underline{p}_h) \in \left(\prod_{k=1}^K X_h^k \right) \times \left(\prod_{k=1}^K \tilde{W}_h^k \right), \\ &\int_{\Gamma^{k,\ell}} ((p_{h,k} + \alpha u_{h,k}) - (-p_{h,\ell} + \alpha u_{h,\ell})) \psi_{h,k,\ell} = 0, \forall \psi_{h,k,\ell} \in \tilde{W}_h^{k,\ell}\}, \end{aligned} \quad (2.7)$$

and the discrete problem is the following one : Find $(\underline{u}_h, \underline{p}_h) \in \mathcal{V}_h$ such that

$$\begin{aligned} \forall \underline{v}_h &= (v_{h,1}, \dots, v_{h,K}) \in \prod_{k=1}^K X_h^k, \\ \sum_{k=1}^K \int_{\Omega^k} (\nabla u_{h,k} \nabla v_{h,k} + u_{h,k} v_{h,k}) dx - \sum_{k=1}^K \int_{\partial\Omega^k} p_{h,k} v_{h,k} ds &= \sum_{k=1}^K \int_{\Omega^k} f_k v_{h,k} dx. \end{aligned} \quad (2.8)$$

The Robin condition (2.7) is the discrete counterpart of (2.6).

3. Iterative algorithm. Let us describe the algorithm in the continuous case, and then in the non conforming discrete case. In both cases, we prove the convergence of the algorithm towards the solution of the problem.

3.1. Continuous case. Let us consider the Robin interface conditions (2.5). We introduce the following notations: $\ll p, v \gg_{\partial\Omega^k} =_{H^{-1/2}(\partial\Omega^k)} \langle p, v \rangle_{H^{1/2}(\partial\Omega^k)}$ and $\langle p, v \rangle_{\Gamma^{k,\ell}} =_{(H_{00}^{1/2}(\Gamma^{k,\ell}))'} \langle p, v \rangle_{H_{00}^{1/2}(\Gamma^{k,\ell})}$. The algorithm is then defined as follows: let $(u_k^n, p_k^n) \in H_*^1(\Omega^k) \times H^{-1/2}(\partial\Omega^k)$ be an approximation of (u, p) in Ω^k at step n . Then, (u_k^{n+1}, p_k^{n+1}) is the solution in $H_*^1(\Omega^k) \times H^{-1/2}(\partial\Omega^k)$ of

$$\int_{\Omega^k} (\nabla u_k^{n+1} \nabla v_k + u_k^{n+1} v_k) dx - \ll p_k^{n+1}, v_k \gg_{\partial\Omega^k} = \int_{\Omega^k} f_k v_k dx, \quad \forall v_k \in H_*^1(\Omega^k), \quad (3.1)$$

$$\langle p_k^{n+1} + \alpha u_k^{n+1}, v_k \rangle_{\Gamma^{k,\ell}} = \langle -p_\ell^n + \alpha u_\ell^n, v_k \rangle_{\Gamma^{k,\ell}}, \quad \forall v_k \in H_{00}^{1/2}(\Gamma^{k,\ell}). \quad (3.2)$$

It is obvious to remark that this series of equations results in uncoupled problems set on every Ω^k . Recalling that $f \in L^2(\Omega)$, the strong formulation is indeed that

$$\begin{aligned} -\Delta u_k^{n+1} + u_k^{n+1} &= f_k && \text{over } \Omega^k \\ \frac{\partial u_k^{n+1}}{\partial \mathbf{n}_k} + \alpha u_k^{n+1} &= -p_\ell^n + \alpha u_\ell^n && \text{over } \Gamma^{k,\ell} \\ p_k^{n+1} &= \frac{\partial u_k^{n+1}}{\partial \mathbf{n}_k} && \text{over } \partial\Omega^k. \end{aligned} \quad (3.3)$$

From this strong formulation it is straightforward to derive by induction that if each p_k^0 , $k = 1, \dots, K$, is chosen in $\prod_\ell H^{1/2}(\Gamma^{k,\ell})$, then, for each k , $1 \leq k \leq K$, and $n \geq 0$ the solution u_k^{n+1} belongs to $H^1(\Omega^k)$ and p_k^{n+1} belongs to $\prod_\ell H^{1/2}(\Gamma^{k,\ell})$ by standard trace results ($p_k^{n+1} = -p_\ell^n + \alpha(u_\ell^n - u_k^{n+1})$). This regularity assumption on p_k^0 will be done hereafter.

We can prove now that the algorithm (3.1)-(3.2) converges for all $f \in L^2(\Omega)$:

THEOREM 1. *Assume that f is in $L^2(\Omega)$ and $(p_k^0)_{1 \leq k \leq K} \in \prod_\ell H^{1/2}(\Gamma^{k,\ell})$. Then, the algorithm (3.1)-(3.2) converges in the sense that*

$$\lim_{n \rightarrow \infty} (\|u_k^n - u_k\|_{H^1(\Omega^k)} + \|p_k^n - p_k\|_{H^{-1/2}(\partial\Omega^k)}) = 0, \quad \text{for } 1 \leq k \leq K,$$

where u_k is the restriction to Ω^k of the solution u to (2.1)-(2.2), and $p_k = \frac{\partial u_k}{\partial \mathbf{n}_k}$ over $\partial\Omega^k$, $1 \leq k \leq K$.

Proof. As the equations are linear, we can take $f = 0$. We prove the convergence in the sense that the associated sequence $(u_k^n, p_k^n)_n$ satisfies

$$\lim_{n \rightarrow \infty} (\|u_k^n\|_{H^1(\Omega^k)} + \|p_k^n\|_{H^{-1/2}(\partial\Omega^k)}) = 0, \quad \text{for } 1 \leq k \leq K.$$

We proceed as in [30, 12] by using an energy estimate that we derive by taking $v_k = u_k^{n+1}$ in (3.1) and the use of the regularity property that $p_k^{n+1} \in L^2(\partial\Omega^k)$

$$\int_{\Omega^k} (|\nabla u_k^{n+1}|^2 + |u_k^{n+1}|^2) dx = \int_{\partial\Omega^k} p_k^{n+1} u_k^{n+1} ds$$

that can also be written

$$\int_{\Omega^k} (|\nabla u_k^{n+1}|^2 + |u_k^{n+1}|^2) dx = \sum_\ell \frac{1}{4\alpha} \int_{\Gamma^{k,\ell}} ((p_k^{n+1} + \alpha u_k^{n+1})^2 - (p_k^{n+1} - \alpha u_k^{n+1})^2) ds.$$

By using the interface conditions (3.2) we obtain

$$\begin{aligned} \int_{\Omega^k} (|\nabla u_k^{n+1}|^2 + |u_k^{n+1}|^2) dx + \frac{1}{4\alpha} \sum_{\ell} \int_{\Gamma^{k,\ell}} (p_k^{n+1} - \alpha u_k^{n+1})^2 ds \\ = \frac{1}{4\alpha} \sum_{\ell} \int_{\Gamma^{k,\ell}} (-p_{\ell}^n + \alpha u_{\ell}^n)^2 ds. \end{aligned} \quad (3.4)$$

Let us now introduce two quantities defined at each step n by :

$$E^n = \sum_{k=1}^K \int_{\Omega^k} (|\nabla u_k^n|^2 + |u_k^n|^2) \quad \text{and} \quad B^n = \frac{1}{4\alpha} \sum_{k=1}^K \sum_{\ell \neq k} \int_{\Gamma^{k,\ell}} (p_k^n - \alpha u_k^n)^2 ds.$$

By summing up the estimates (3.4) over $k = 1, \dots, K$, we have $E^{n+1} + B^{n+1} \leq B^n$, so that, by summing up these inequalities, now over n , we obtain :

$$\sum_{n=1}^{\infty} E^n \leq B^0.$$

We thus have $\lim_{n \rightarrow \infty} E^n = 0$. Relation (3.3) then implies :

$$\lim_{n \rightarrow \infty} \|p_k^n\|_{H^{-1/2}(\partial\Omega^k)} = 0, \quad \text{for } k = 1, \dots, K,$$

which ends the proof of the convergence of the continuous algorithm. \square

3.2. Discrete case. We first introduce the discrete algorithm defined by: let $(u_{h,k}^n, p_{h,k}^n) \in X_h^k \times \tilde{W}_h^k$ be a discrete approximation of (u, p) in Ω^k at step n . Then, $(u_{h,k}^{n+1}, p_{h,k}^{n+1})$ is the solution in $X_h^k \times \tilde{W}_h^k$ of

$$\int_{\Omega^k} \left(\nabla u_{h,k}^{n+1} \nabla v_{h,k} + u_{h,k}^{n+1} v_{h,k} \right) dx - \int_{\partial\Omega^k} p_{h,k}^{n+1} v_{h,k} ds = \int_{\Omega^k} f_k v_{h,k} dx, \quad \forall v_{h,k} \in X_h^k, \quad (3.5)$$

$$\int_{\Gamma^{k,\ell}} (p_{h,k}^{n+1} + \alpha u_{h,k}^{n+1}) \psi_{h,k,\ell} = \int_{\Gamma^{k,\ell}} (-p_{h,\ell}^n + \alpha u_{h,\ell}^n) \psi_{h,k,\ell}, \quad \forall \psi_{h,k,\ell} \in \tilde{W}_h^{k,\ell}. \quad (3.6)$$

In order to analyze the convergence of this iterative scheme, we have to precise the norms that can be used on the Lagrange multipliers \underline{p}_h . For any $\underline{p} \in \prod_{k=1}^K L^2(\partial\Omega^k)$, in addition to the natural L^2 norm, we can define two better suited norms as follows

$$\|\underline{p}\|_{-\frac{1}{2}} = \left(\sum_{k=1}^K \|p_k\|_{H^{-\frac{1}{2}}(\partial\Omega^k)}^2 \right)^{\frac{1}{2}} \quad \text{and} \quad \|\underline{p}\|_{-\frac{1}{2},*} = \left(\sum_{k=1}^K \sum_{\substack{\ell=1 \\ \ell \neq k}}^K \|p_k\|_{H_*^{-\frac{1}{2}}(\Gamma^{k,\ell})}^2 \right)^{\frac{1}{2}},$$

where $\|\cdot\|_{H_*^{-\frac{1}{2}}(\Gamma^{k,\ell})}$ stands for the dual norm of $H_{00}^{\frac{1}{2}}(\Gamma^{k,\ell})$. We also need a stability result for the Lagrange multipliers, and refer to [5] in 2D and to [25] in 3D, in which it is shown that,

LEMMA 1. *There exists a constant c_* such that, for any $p_{h,k,\ell}$ in $\tilde{W}_h^{k,\ell}$, there exists an element $w^{h,k,\ell}$ in X_h^k that vanishes over $\partial\Omega^k \setminus \Gamma^{k,\ell}$ and satisfies*

$$\int_{\Gamma^{k,\ell}} p_{h,k,\ell} w^{h,k,\ell} \geq \|p_{h,k,\ell}\|_{H_*^{-\frac{1}{2}}(\Gamma^{k,\ell})}^2 \quad (3.7)$$

with a bounded norm

$$\|w^{h,k,\ell}\|_{H^1(\Omega^k)} \leq c_* \|p_{h,k,\ell}\|_{H_*^{-\frac{1}{2}}(\Gamma^{k,\ell})}.$$

Let $\pi_{k,\ell}$ denote the orthogonal projection operator from $L^2(\Gamma^{k,\ell})$ onto $\tilde{W}_h^{k,\ell}$. Then, for $v \in L^2(\Gamma^{k,\ell})$, $\pi_{k,\ell}(v)$ is the unique element of $\tilde{W}_h^{k,\ell}$ such that

$$\int_{\Gamma^{k,\ell}} (\pi_{k,\ell}(v) - v)\psi = 0, \quad \forall \psi \in \tilde{W}_h^{k,\ell}. \quad (3.8)$$

We are now in a position to prove the convergence of the iterative scheme

THEOREM 2. *Let us assume that $\alpha h \leq c$, for some small enough constant c . Then, the discrete problem (2.8) has a unique solution $(\underline{u}_h, \underline{p}_h) \in \mathcal{V}_h$. The algorithm (3.5)-(3.6) is well posed and converges in the sense that*

$$\lim_{n \rightarrow \infty} \left(\|u_{h,k}^n - u_{h,k}\|_{H^1(\Omega^k)} + \sum_{\ell \neq k} \|p_{h,k,\ell}^n - p_{h,k,\ell}\|_{H_*^{-\frac{1}{2}}(\Gamma^{k,\ell})} \right) = 0, \text{ for } 1 \leq k \leq K.$$

Proof. For the sake of convenience, we drop out the index h in what follows. We first assume that problems (2.8) and (3.5)-(3.6) are well posed and proceed as in the continuous case and assume that $f = 0$. From (3.8) we have

$$\forall v_k \in L^2(\Gamma^{k,\ell}), \quad \int_{\Gamma^{k,\ell}} p_k^{n+1} v_k = \int_{\Gamma^{k,\ell}} p_k^{n+1} \pi_{k,\ell}(v_k),$$

and (3.6) also reads

$$p_k^{n+1} + \alpha \pi_{k,\ell}(u_k^{n+1}) = \pi_{k,\ell}(-p_\ell^n + \alpha u_\ell^n) \quad \text{over } \Gamma^{k,\ell}. \quad (3.9)$$

By taking $v_k = u_k^{n+1}$ in (3.5), we thus have

$$\begin{aligned} & \int_{\Omega^k} (|\nabla u_k^{n+1}|^2 + |u_k^{n+1}|^2) dx \\ &= \sum_{\ell} \frac{1}{4\alpha} \int_{\Gamma^{k,\ell}} ((p_k^{n+1} + \alpha \pi_{k,\ell}(u_k^{n+1}))^2 - (p_k^{n+1} - \alpha \pi_{k,\ell}(u_k^{n+1}))^2) ds. \end{aligned}$$

Then, by using the interface conditions (3.9) we obtain

$$\begin{aligned} & \int_{\Omega^k} (|\nabla u_k^{n+1}|^2 + |u_k^{n+1}|^2) dx + \frac{1}{4\alpha} \sum_{\ell} \int_{\Gamma^{k,\ell}} (p_k^{n+1} - \alpha \pi_{k,\ell}(u_k^{n+1}))^2 ds \\ &= \frac{1}{4\alpha} \sum_{\ell} \int_{\Gamma^{k,\ell}} (\pi_{k,\ell}(p_\ell^n - \alpha u_\ell^n))^2 ds. \end{aligned}$$

It is straightforward to note that

$$\begin{aligned} & \int_{\Gamma^{k,\ell}} (\pi_{k,\ell}(p_\ell^n - \alpha u_\ell^n))^2 ds \leq \int_{\Gamma^{k,\ell}} (p_\ell^n - \alpha u_\ell^n)^2 ds \\ &= \int_{\Gamma^{k,\ell}} (p_\ell^n - \alpha \pi_{\ell,k}(u_\ell^n) + \alpha \pi_{\ell,k}(u_\ell^n) - \alpha u_\ell^n)^2 ds \\ &= \int_{\Gamma^{k,\ell}} (p_\ell^n - \alpha \pi_{\ell,k}(u_\ell^n))^2 + \alpha^2 (\pi_{\ell,k}(u_\ell^n) - u_\ell^n)^2 ds \end{aligned}$$

since $(Id - \pi_{\ell,k})(u_\ell^n)$ is orthogonal to any element in $\tilde{W}_h^{\ell,k}$. For the last term above, we recall that (see [8] in 2D and [6] or [9] equation (5.1) in 3D)

$$\int_{\Gamma^{k,\ell}} (\pi_{\ell,k}(u_\ell^n) - u_\ell^n)^2 ds \leq ch \|u_\ell^n\|_{H^{1/2}(\Gamma^{k,\ell})}^2 \leq ch \|u_\ell^n\|_{H^1(\Omega^\ell)}^2.$$

With similar notations as those introduced in the continuous case, we deduce

$$E^{n+1} + B^{n+1} \leq c\alpha h E^n + B^n$$

and we conclude as in the continuous case: if $c\alpha h < 1$ then $\lim_{n \rightarrow \infty} E^n = 0$. The convergence of u_k^n towards 0 in the H^1 norm follows. Taking $f = 0$ in (3.5), then using (3.7) and the convergence of u_k^n towards 0 in the H^1 norm, we derive the convergence of p_k^n in the $H_*^{-\frac{1}{2}}(\Gamma^{k,\ell})$ norm. Note that by having $f = 0$ and $(u^n, p^n) = 0$ prove that $(u^{n+1}, p^{n+1}) = 0$ from which we derive that the square problem (3.5)-(3.6) is uniquely solvable hence well posed. Similarly, having $f = 0$ and getting rid of the superscripts n and $n + 1$ in the previous proof gives (with obvious notations) :

$$E + B \leq c\alpha h E + B.$$

The existence and uniqueness of a solution of (2.8) then results with similar arguments.

In [25] the well-posedness of (2.8) is addressed through a more direct proof: let us introduce over $(\prod_{k=1}^K H_*^1(\Omega^k) \times \prod_{k=1}^K L^2(\partial\Omega^k)) \times \prod_{k=1}^K H_*^1(\Omega^k)$ the bilinear form

$$\tilde{a}(\underline{u}, \underline{p}, \underline{v}) = \sum_{k=1}^K \int_{\Omega^k} (\nabla u_k \nabla v_k + u_k v_k) dx - \sum_{k=1}^K \int_{\partial\Omega^k} p_k v_k ds.$$

The space $\prod_{k=1}^K H_*^1(\Omega^k)$ is endowed with the norm

$$\|\underline{v}\|_* = \left(\sum_{k=1}^K \|v_k\|_{H^1(\Omega^k)}^2 \right)^{\frac{1}{2}}.$$

LEMMA 2. *There exists $c' > 0$ and a constant $\beta > 0$ such that*

$$\begin{aligned} \text{for } \alpha h \leq c', \quad \forall (\underline{u}_h, \underline{p}_h) \in \mathcal{V}_h, \quad \exists \underline{v}_h \in \prod_{k=1}^K X_h^k, \\ \tilde{a}((\underline{u}_h, \underline{p}_h), \underline{v}_h) \geq \beta (\|\underline{u}_h\|_* + \|\underline{p}_h\|_{-\frac{1}{2},*}) \|\underline{v}_h\|_*. \end{aligned}$$

Moreover, we have the continuity argument : there exists a constant $c > 0$ such that

$$\forall (\underline{u}_h, \underline{p}_h) \in \mathcal{V}_h, \quad \forall \underline{v}_h \in \prod_{k=1}^K X_h^k, \quad \tilde{a}((\underline{u}_h, \underline{p}_h), \underline{v}_h) \leq c (\|\underline{u}_h\|_* + \|\underline{p}_h\|_{-\frac{1}{2}}) (\|\underline{v}_h\|_*). \quad (3.10)$$

This lemma is proven in [25], based on Lemma 1. From Lemma 2, we have for any $(\tilde{\underline{u}}_h, \tilde{\underline{p}}_h) \in \mathcal{V}_h$,

$$\|\underline{u} - \underline{u}_h\|_* + \|\underline{p} - \underline{p}_h\|_{-\frac{1}{2},*} \leq c (\|\underline{u} - \tilde{\underline{u}}_h\|_* + \|\underline{p} - \tilde{\underline{p}}_h\|_{-\frac{1}{2}}). \quad (3.11)$$

and we are led to the analysis of the best fit of $(\underline{u}, \underline{p})$ by elements in \mathcal{V}_h .

As noticed in [25], it is well known [5, 9] but unusual that the inf-sup and continuity conditions involve different norms: the $\|\cdot\|_{-\frac{1}{2}}$ and $\|\cdot\|_{-\frac{1}{2},*}$ norms. Thus, these two different norms appear in (3.11) and the best approximation analysis will be done using the $\|\cdot\|_{-\frac{1}{2}}$ norm, while the error estimates will involve the $\|\cdot\|_{-\frac{1}{2},*}$ norm.

The analysis of the best fit as been done in [25] in 2D and 3D for \mathbf{P}_1 approximations. Let us analyze the best approximation of $(\underline{u}, \underline{p})$ by elements in \mathcal{V}_h in the general case of higher order approximations in 2D.

4. Analysis of the best fit in 2D for higher order approximations. In this part we analyze the best approximation of $(\underline{u}, \underline{p})$ by elements in \mathcal{V}_h .

Following the same lines as in the analysis of the best fit in the \mathbf{P}_1 situation of [25], we can prove the following results:

THEOREM 3. *Let $u \in H^2(\Omega) \cap H_0^1(\Omega)$, be such that $\underline{u} = (u_k)_{1 \leq k \leq K} \in \prod_{k=1}^K H^{2+m}(\Omega^k)$ with $u_k = u|_{\Omega^k}$, and $p - 1 \geq m \geq 0$. Let us set also $p_{k,\ell} = \frac{\partial u}{\partial \mathbf{n}_k}$ over each $\Gamma^{k,\ell}$. Then there exists $\tilde{\underline{u}}_h$ in $\prod_{k=1}^K X_h^k$ and $\tilde{\underline{p}}_h = (\tilde{p}_{k\ell h})$, with $\tilde{p}_{k\ell h} \in \tilde{W}_h^{k,\ell}$ such that $(\tilde{\underline{u}}_h, \tilde{\underline{p}}_h)$ satisfy the coupling condition (2.7), and*

$$\|\tilde{\underline{u}}_h - \underline{u}\|_* \leq ch^{1+m} \sum_{k=1}^K \|u_k\|_{H^{2+m}(\Omega^k)} + \frac{ch^m}{\alpha} \sum_{\ell=1}^K \sum_{k<\ell} \|p_{k,\ell}\|_{H^{\frac{1}{2}+m}(\Gamma^{k,\ell})},$$

$$\begin{aligned} \|\tilde{p}_{k\ell h} - p_{k,\ell}\|_{H^{-\frac{1}{2}}(\Gamma^{k,\ell})} &\leq c\alpha h^{2+m} (\|u_k\|_{H^{2+m}(\Omega^k)} + \|u_\ell\|_{H^{2+m}(\Omega^\ell)}) \\ &\quad + ch^{1+m} \|p_{k,\ell}\|_{H^{\frac{1}{2}+m}(\Gamma^{k,\ell})}. \end{aligned}$$

where c is a constant independent of h and α .

If we assume more regularity on the normal derivatives on the interfaces, we have

THEOREM 4. *Under the assumptions of Theorem 3 and assuming in addition that $p_{k,\ell}$ is in $H^{\frac{3}{2}+m}(\Gamma^{k,\ell})$. Then there exists $\tilde{\underline{u}}_h$ in $\prod_{k=1}^K X_h^k$ and $\tilde{\underline{p}}_h = (\tilde{p}_{k\ell h})$, $\tilde{p}_{k\ell h} \in \tilde{W}_h^{k,\ell}$ such that $(\tilde{\underline{u}}_h, \tilde{\underline{p}}_h)$ satisfy (2.7), and*

$$\begin{aligned} \|\tilde{\underline{u}}_h - \underline{u}\|_* &\leq ch^{1+m} \sum_{k=1}^K \|u_k\|_{H^{2+m}(\Omega^k)} + \frac{ch^{m+1}}{\alpha} (\log h)^{\beta(m)} \sum_{\ell=1}^K \sum_{k<\ell} \|p_{k,\ell}\|_{H^{\frac{3}{2}+m}(\Gamma^{k,\ell})}, \\ \|\tilde{p}_{k\ell h} - p_{k,\ell}\|_{H^{-\frac{1}{2}}(\Gamma^{k,\ell})} &\leq c\alpha h^{2+m} (\|u_k\|_{H^{2+m}(\Omega^k)} + \|u_\ell\|_{H^{2+m}(\Omega^\ell)}) \\ &\quad + ch^{2+m} (\log h)^{\beta(m)} \|p_{k,\ell}\|_{H^{\frac{3}{2}+m}(\Gamma^{k,\ell})}. \end{aligned}$$

where c is a constant independent of h and α , and $\beta(m) = 0$ if $m \leq p - 2$ and $\beta(m) = 1$ if $m = p - 1$.

The main part of the proof is independent of the degree of the approximation and is done in [25]. Only Lemma 4 in [25] is dependent of the degree of the approximation and is only proven for a \mathbf{P}_1 approximation. We prove it for higher order approximations:

LEMMA 3. *Assume the degree of the finite element approximation $p \leq 13$. There exists two constants $c_1 > 0$ and $c_2 > 0$ independent of h such that for all $\eta_{\ell,k}$ in $\mathcal{Y}_h^{\ell,k} \cap H_0^1(\Gamma^{k,\ell})$, there exists an element $\psi_{\ell,k}$ in $\tilde{W}_h^{\ell,k}$, such that*

$$\int_{\Gamma^{k,\ell}} (\eta_{\ell,k} + \pi_{k,\ell}(\eta_{\ell,k})) \psi_{\ell,k} \geq c_1 \|\eta_{\ell,k}\|_{L^2(\Gamma^{k,\ell})}^2, \quad (4.1)$$

$$\|\psi_{\ell,k}\|_{L^2(\Gamma^{k,\ell})} \leq c_2 \|\eta_{\ell,k}\|_{L^2(\Gamma^{k,\ell})}. \quad (4.2)$$

REMARK 1. *The limit $p \leq 13$ is related to the arguments used in the proof we propose for this lemma, thus, a priori, only technical. We have not found how to alleviate this limit but actually, for applications, this limit is quite above what is generally admitted as the optimal range for the degree of the polynomial in $h - P$ finite element methods. Indeed, as regards the question of accuracy with respect to run time, the publication [37] analyses in full details¹ and on a variety of problems and regularity of solutions, the accuracy achieved by low to high order finite element approximations as a function of the number of degrees of freedom and of the run time. It appears that the use of degrees between 5 and 8 is quite competitive which motivates the present analysis.*

The proof of these results is performed in the following steps. Note that Lemma 4 below, that generalizes one of the main arguments in the proof of Lemma 4 in [25] to higher degree in 2d would involve, for a similar generalization in 3d (see Lemma 7 of [25]), an extension to higher order of the theory developed in [9] that does not exist yet and goes beyond the scope of the present paper.

4.1. A first technical result.

LEMMA 4. *Let $1 \leq p \leq 13$ be an integer. There exists c and $C > 0$ such that for all $\eta \in \mathbf{P}_p([-1, 1])$ s.t. $\eta(-1) = 0$ there exists $\psi \in \mathbf{P}_{p-1}([-1, 1])$ s.t. $\eta(1) = \psi(1)$, and*

$$J(\psi; \eta) := \int_{-1}^1 (\eta \psi - \frac{1}{4}(\eta - \psi)^2) \geq c \int_{-1}^1 \eta^2 \quad \text{and} \quad \int_{-1}^1 \psi^2 \leq C \int_{-1}^1 \eta^2.$$

Proof. This lemma has been proven in the case $p = 1$ in [25]. For $p \geq 2$, we prove it by studying for a given $\eta \in \mathbf{P}_p([-1, 1])$, $\eta \neq 0$ the maximization problem :

Find $\psi \in \mathbf{P}_{p-1}([-1, 1])$ such that

$$J(\psi; \eta) = \max_{\substack{\varphi \in \mathbf{P}_{p-1}([-1, 1]) \\ \varphi(1) = \eta(1)}} J(\varphi; \eta). \quad (4.3)$$

The function J is strictly concave in φ and there exists a function satisfying the constraint. This problem admits a solution. The functional $J(\varphi, \eta)$ being quadratic in (φ, η) and the constraint being affine, the optimality condition shows that the problem reduces to a linear problem the right hand side of which depends linearly of η . The affine constraint being of rank one, the problem (4.3) admits a unique solution which depends linearly of η . Therefore, it makes sense to introduce the operator:

$$S : \mathbf{P}_{p,0}([-1, 1]) \longrightarrow \mathbf{P}_{p-1}([-1, 1]) \\ \eta \longmapsto \psi \text{ solution to (4.3),}$$

where $\mathbf{P}_{p,0}([-1, 1])$ is the set of functions of $\mathbf{P}_p([-1, 1])$ that vanish at -1 . In Lemma 4, we take $\psi = S(\eta)$. The operator S is linear from a finite dimensional space to another so that it is continuous for any norm on these spaces. Therefore

¹Of course the answer to that question depends on the implementation of the discretization method and the exact properties of the solution to be approximated but this indicates a tendency that is confirmed by implementation on a large set of other applications.

there exists $C > 0$ possibly depending on p such that $\int_{-1}^1 \psi^2 \leq C \int_{-1}^1 \eta^2$. Moreover, the function

$$\begin{aligned} H : \mathbf{P}_{p,0}([-1,1]) \setminus \{0\} &\longrightarrow \mathbb{R} \\ \eta &\longmapsto \frac{J(S(\eta), \eta)}{\int_{-1}^1 \eta^2} \end{aligned}$$

is continuous and such that $H(\eta) = H(\alpha\eta)$ for any $\alpha \neq 0$. Therefore, it reaches its minimum which is strictly positive as results from the lemma stated and proven in the next subsection and the proof of Lemma 4 is complete. \square

4.2. Another technical result.

LEMMA 5. *Let $p \leq 13$ and $\eta \in \mathbf{P}_p([-1,1])$ s.t. $\eta(-1) = 0$ and η is not the null function. Then, $J(S(\eta); \eta) > 0$.*

Proof. We make use of the Legendre polynomials

$$L_0(x) = 1, \quad L_1(x) = x, \quad (m+1)L_{m+1}(x) = (2m+1)xL_m(x) - mL_{m-1}(x), \quad m \geq 1.$$

Let us recall that for any $m \geq 0$,

$$L_m(1) = 1, \quad L_m(-1) = (-1)^m, \quad \int_{-1}^1 L_m(x) L_{m'}(x) dx = \delta_{mm'} \frac{2}{2m+1}.$$

The polynomial η is decomposed on the Legendre polynomials

$$\eta = \sum_{m=1}^p \eta_m (L_m + L_{m-1}),$$

and $\psi = S(\eta)$ is sought in the form

$$\psi = \sum_{m=0}^{p-1} \psi_m L_m$$

so that it maximizes the quantity $J(\psi; \eta)$ under the constraint $\eta(1) = \psi(1)$. This corresponds to the min-max problem

$$\max_{\psi \in \mathbf{P}_{p-1}([-1,1])} \min_{\mu \in \mathbb{R}} \mathcal{L}(\psi, \mu)$$

where

$$\mathcal{L}(\psi, \mu) = J(\psi; \eta) - \mu(\psi(1) - \eta(1)).$$

We have to prove that the optimal value is positive. The optimality relations w.r.t ψ give

$$\frac{3}{2}(\eta_m + \eta_{m+1}) - \frac{1}{2}\psi_m = \mu \frac{2m+1}{2}, \quad 1 \leq m \leq p-1, \quad \frac{3}{2}\eta_1 - \frac{1}{2}\psi_0 = \frac{\mu}{2}.$$

Denoting $R_{p-1} = \sum_{m=0}^{p-1} (2m+1)L_m$, with $\|R_{p-1}\|_{L^2([-1,1])}^2 = 2p^2$, we get

$$\psi = 3\eta - 3\eta_p L_p - \mu R_{p-1}. \tag{4.4}$$

Hence, the dual problem writes

$$\min_{\mu \in \mathbb{R}} G(\mu; \eta),$$

where $G(\mu; \eta) := J(3\eta - 3\eta_p L_p - \mu R_{p-1}; \eta) - \mu(\psi(1) - \eta(1))$ and ψ satisfies (4.4). After some calculations, $G(\mu; \eta)$ appears a second order polynomial in μ :

$$G(\mu; \eta) = \frac{p^2}{2}\mu^2 - \mu(2\eta(1) - 3\eta_p) + (2\|\eta\|_{L^2([-1,1])}^2 - \frac{9}{2}\frac{\eta_p^2}{2p+1}); \quad (4.5)$$

its leading coefficient is positive and its discriminant is proven to be negative in the next lemma, from which we derive that $\min_{\mu} G(\mu; \eta)$ is positive and the proof is complete. \square

LEMMA 6. For $p \leq 13$, the discriminant of (4.5):

$$\Delta(\eta) := (2\eta(1) - 3\eta_p)^2 + p^2(-4\|\eta\|_{L^2([-1,1])}^2 + 9\frac{\eta_p^2}{2p+1})$$

is negative if $\eta \in \mathbf{P}_p([-1, 1])$, $\eta(-1) = 0$ and η is not the null function.

Proof of Lemma 6 in the the case $p = 2$. (the proof for $3 \leq p \leq 13$, is given in Appendix A).

For $p = 2$, a direct computation shows that

$$\Delta(\eta) = -\frac{80}{3}\eta_1^2 - \frac{40}{3}\eta_2\eta_1 - \frac{133}{15}\eta_2^2.$$

The discriminant of the corresponding bilinear form is $-8632/9$. It is negative and the lemma is proven in this case. \square

4.3. Proof of Lemma 3. Using the definition of $\pi_{k,\ell}$, (3.8), we derive

$$\int_{\Gamma^{k,\ell}} (\eta_{\ell,k} + \pi_{k,\ell}(\eta_{\ell,k}))\psi_{\ell,k} = \int_{\Gamma^{k,\ell}} \eta_{\ell,k}\psi_{\ell,k} + \int_{\Gamma^{k,\ell}} (\pi_{k,\ell}(\eta_{\ell,k}))^2 + \int_{\Gamma^{k,\ell}} \pi_{k,\ell}(\eta_{\ell,k})(\psi_{\ell,k} - \eta_{\ell,k}).$$

Then, using the relation $\pi_{k,\ell}(\eta_{\ell,k})(\psi_{\ell,k} - \eta_{\ell,k}) \geq -(\pi_{k,\ell}(\eta_{\ell,k}))^2 - \frac{1}{4}(\psi_{\ell,k} - \eta_{\ell,k})^2$ leads to

$$\int_{\Gamma^{k,\ell}} (\eta_{\ell,k} + \pi_{k,\ell}(\eta_{\ell,k}))\psi_{\ell,k} \geq \int_{\Gamma^{k,\ell}} \eta_{\ell,k}\psi_{\ell,k} - \frac{1}{4} \int_{\Gamma^{k,\ell}} (\psi_{\ell,k} - \eta_{\ell,k})^2.$$

Remind that we have denoted as $x_0^{\ell,k}, x_1^{\ell,k}, \dots, x_{N-1}^{\ell,k}, x_N^{\ell,k}$ the vertices of the triangulation of $\Gamma^{\ell,k}$ that belong to $\Gamma^{\ell,k}$. By Lemma 4, and an easy scaling argument, there exists $c, C > 0$, $\psi_1 \in \mathbf{P}_{p-1}([x_0^{\ell,k}, x_1^{\ell,k}])$, and $\psi_N \in \mathbf{P}_{p-1}([x_{N-1}^{\ell,k}, x_N^{\ell,k}])$, such that

$$\|\psi_1\|_{L^2(x_0^{\ell,k}, x_1^{\ell,k})} + \|\psi_N\|_{L^2(x_{N-1}^{\ell,k}, x_N^{\ell,k})} \leq C(\|\eta_{\ell,k}\|_{L^2(x_0^{\ell,k}, x_1^{\ell,k})} + \|\eta_{\ell,k}\|_{L^2(x_{N-1}^{\ell,k}, x_N^{\ell,k})}),$$

$\psi_1(x_1^{\ell,k}) = \eta_{\ell,k}(x_1^{\ell,k})$, $\psi_N(x_{N-1}^{\ell,k}) = \eta_{\ell,k}(x_{N-1}^{\ell,k})$ and

$$\int_{x_0^{\ell,k}}^{x_1^{\ell,k}} (\eta_{\ell,k}\psi_1 - \frac{1}{4}(\psi_1 - \eta_{\ell,k})^2) + \int_{x_{N-1}^{\ell,k}}^{x_N^{\ell,k}} (\eta_{\ell,k}\psi_N - \frac{1}{4}(\psi_N - \eta_{\ell,k})^2) \geq c(\int_{x_0^{\ell,k}}^{x_1^{\ell,k}} \eta_{\ell,k}^2 + \int_{x_{N-1}^{\ell,k}}^{x_N^{\ell,k}} \eta_{\ell,k}^2).$$

Taking $\psi_{\ell,k}$ in $\tilde{W}_h^{\ell,k}$ as follows

$$\psi_{\ell,k} = \begin{cases} \psi_1 & \text{over }]x_0^{\ell,k}, x_1^{\ell,k}[\\ \eta_{\ell,k} & \text{over }]x_1^{\ell,k}, x_{N-1}^{\ell,k}[\\ \psi_N & \text{over }]x_{N-1}^{\ell,k}, x_N^{\ell,k}[\end{cases}$$

proves Lemma 3 with $c_1 = \min(1, c)$ and $c_2 = \max(1, C)$. \square

4.4. Proof of Theorem 3. We follow the same steps as in the proof of Theorem 2 in [25]. Let u_{kh}^1 be the unique element of X_h^k defined as follows :

- $(u_{kh}^1)|_{\partial\Omega^k}$ is the best fit of u_k over $\partial\Omega^k$ in $\mathcal{Y}_h^{k,\ell}$,
- u_{kh}^1 at the inner nodes of the triangulation (in Ω^k) coincide with the interpolate of u_k .

Then, it satisfies, for $0 \leq m \leq p-1$,

$$\|u_{kh}^1 - u_k\|_{L^2(\partial\Omega^k)} \leq ch^{\frac{3}{2}+m} \|u_k\|_{H^{2+m}(\Omega^k)}, \quad (4.6)$$

from which we deduce that

$$\|u_{kh}^1 - u_k\|_{L^2(\Omega^k)} + h \|u_{kh}^1 - u_k\|_{H^1(\Omega^k)} \leq ch^{2+m} \|u_k\|_{H^{2+m}(\Omega^k)}, \quad (4.7)$$

and, from Aubin-Nitsche estimate,

$$\|u_{kh}^1 - u_k\|_{H^{-\frac{1}{2}}(\Gamma^{k,\ell})} \leq ch^{2+m} \|u_k\|_{H^{2+m}(\Omega^k)}. \quad (4.8)$$

We introduce separately the best fit $p_{k\ell h}^1$ of $p_{k,\ell} = \frac{\partial u}{\partial \mathbf{n}_k}$ over each $\Gamma^{k,\ell}$ in $\tilde{W}_h^{k,\ell}$. Then we have, for $0 \leq m \leq p-1$

$$\|p_{k\ell h}^1 - p_{k,\ell}\|_{L^2(\Gamma^{k,\ell})} \leq ch^{\frac{1}{2}+m} \|p_{k,\ell}\|_{H^{\frac{1}{2}+m}(\Gamma^{k,\ell})}, \quad (4.9)$$

$$\|p_{k\ell h}^1 - p_{k,\ell}\|_{H^{-\frac{1}{2}}(\Gamma^{k,\ell})} \leq ch^{1+m} \|p_{k,\ell}\|_{H^{\frac{1}{2}+m}(\Gamma^{k,\ell})}. \quad (4.10)$$

But there is very few chance that $(\underline{u}_h, \underline{p}_h^1) \in \left(\prod_{k=1}^K X_h^k\right) \times \left(\prod_{k=1}^K \tilde{W}_h^k\right)$ satisfy the coupling condition (2.7). It misses (2.7) of elements $\epsilon_{k,\ell}$ and $\eta_{\ell,k}$ such that

$$\int_{\Gamma^{k,\ell}} (p_{k\ell h}^1 + \epsilon_{k,\ell} + \alpha u_{kh}^1) \psi_{k,\ell} = \int_{\Gamma^{k,\ell}} (-p_{\ell kh}^1 + \alpha \eta_{\ell,k} + \alpha u_{\ell h}^1) \psi_{k,\ell}, \quad \forall \psi_{k,\ell} \in \tilde{W}_h^{k,\ell} \quad (4.11)$$

$$\int_{\Gamma^{k,\ell}} (p_{\ell kh}^1 + \alpha \eta_{\ell,k} + \alpha u_{\ell h}^1) \psi_{\ell,k} = \int_{\Gamma^{k,\ell}} (-p_{k\ell h}^1 - \epsilon_{k,\ell} + \alpha u_{kh}^1) \psi_{\ell,k}, \quad \forall \psi_{\ell,k} \in \tilde{W}_h^{\ell,k}. \quad (4.12)$$

In order to correct that, without polluting (4.6)-(4.10), for each couple (k, ℓ) we choose one side, e.g. the smaller indexed one (hereafter we shall assume that each couple (k, ℓ) is ordered by $k < \ell$). With this choice, we introduce $\epsilon_{k,\ell} \in \tilde{W}_h^{k,\ell}$, $\eta_{\ell,k} \in \mathcal{Y}_h^{\ell,k} \cap H_0^1(\Gamma^{k,\ell})$ such that the element $(\tilde{u}_h, \tilde{p}_h)$, defined by

$$\tilde{u}_{\ell h} = u_{\ell h}^1 + \sum_{k < \ell} \mathcal{R}_{\ell,k}(\eta_{\ell,k}), \quad \tilde{p}_{k\ell h} = p_{k\ell h}^1 + \epsilon_{k,\ell} \quad (\text{for } k < \ell), \quad (4.13)$$

satisfy (2.7). Here $\mathcal{R}_{\ell,k}$ is a discrete lifting operator as in [25] (see also [38, 7]) that satisfies, with a constant c that is h -independent, that vanishes over $\partial\Omega^\ell \setminus \Gamma^{k,\ell}$ and satisfies

$$\forall w \in \mathcal{Y}_h^{\ell,k} \cap H_0^1(\Gamma^{k,\ell}), \quad (\mathcal{R}_{\ell,k}(w))|_{\Gamma^{k,\ell}} = w, \quad \|\mathcal{R}_{\ell,k}(w)\|_{H^1(\Omega^\ell)} \leq c \|w\|_{H_0^{\frac{1}{2}}(\Gamma^{k,\ell})} \quad (4.14)$$

The set of equations (4.11)-(4.12) results in a square system of linear algebraic equations for $\epsilon_{k,\ell}$ and $\eta_{\ell,k}$ that can be written as follows

$$\int_{\Gamma^{k,\ell}} (\epsilon_{k,\ell} - \alpha \eta_{\ell,k}) \psi_{k,\ell} = \int_{\Gamma^{k,\ell}} e_1 \psi_{k,\ell}, \quad \forall \psi_{k,\ell} \in \tilde{W}_h^{k,\ell} \quad (4.15)$$

$$\int_{\Gamma^{k,\ell}} (\epsilon_{k,\ell} + \alpha \eta_{\ell,k}) \psi_{\ell,k} = \int_{\Gamma^{k,\ell}} e_2 \psi_{\ell,k}, \quad \forall \psi_{\ell,k} \in \tilde{W}_h^{\ell,k}, \quad (4.16)$$

with

$$e_1 = -p_{k\ell h}^1 - p_{\ell kh}^1 + \alpha(u_{\ell h}^1 - u_{kh}^1), \quad e_2 = -p_{k\ell h}^1 - p_{\ell kh}^1 + \alpha(u_{kh}^1 - u_{\ell h}^1). \quad (4.17)$$

In [25], it is shown that the linear system (4.15)-(4.16) is well posed.

We now estimate $\|\tilde{p}_{k\ell h} - p_{k,\ell}\|_{H^{-\frac{1}{2}}(\Gamma^{k,\ell})}$ and $\|\tilde{u}_{\ell h} - u_\ell\|_{H^1(\Omega^\ell)}$, by first estimating $\|\eta_{\ell,k}\|_{L^2(\Gamma^{k,\ell})}$: from (4.15) and (4.16), we get

$$\epsilon_{k,\ell} = \pi_{k,\ell}(\alpha\eta_{\ell,k} + e_1), \quad \alpha\eta_{\ell,k} = \pi_{\ell,k}(-\epsilon_{k,\ell} + e_2). \quad (4.18)$$

Injecting the first equation of (4.18) in (4.15)-(4.16), we obtain

$$\int_{\Gamma^{k,\ell}} (\eta_{\ell,k} + \pi_{k,\ell}(\eta_{\ell,k}))\psi_{\ell,k} = \frac{1}{\alpha} \int_{\Gamma^{k,\ell}} (e_2 - \pi_{k,\ell}(e_1))\psi_{\ell,k}, \quad \forall \psi_{\ell,k} \in \tilde{W}_h^{\ell,k}. \quad (4.19)$$

Then, from (4.1) and (4.19) we get

$$c_1 \|\eta_{\ell,k}\|_{L^2(\Gamma^{k,\ell})}^2 \leq \frac{1}{\alpha} \|e_2 - \pi_{k,\ell}(e_1)\|_{L^2(\Gamma^{k,\ell})} \|\psi_{\ell,k}\|_{L^2(\Gamma^{k,\ell})}, \quad (4.20)$$

and using (4.2) in (4.20) yields

$$\|\eta_{\ell,k}\|_{L^2(\Gamma^{k,\ell})} \leq \frac{c_2}{\alpha c_1} \|e_2 - \pi_{k,\ell}(e_1)\|_{L^2(\Gamma^{k,\ell})} \leq \frac{c_2}{\alpha c_1} (\|e_2\|_{L^2(\Gamma^{k,\ell})} + \|e_1\|_{L^2(\Gamma^{k,\ell})}). \quad (4.21)$$

Now, from (4.17), for $i = 1, 2$

$$\|e_i\|_{L^2(\Gamma^{k,\ell})} \leq \|p_{k\ell h}^1 + p_{\ell kh}^1\|_{L^2(\Gamma^{k,\ell})} + \alpha \|u_{\ell h}^1 - u_{kh}^1\|_{L^2(\Gamma^{k,\ell})},$$

and recalling that $p_{k,\ell} = \frac{\partial u_k}{\partial \mathbf{n}_k} = -\frac{\partial u_\ell}{\partial \mathbf{n}_\ell} = -p_{\ell,k}$ over each $\Gamma^{k,\ell}$

$$\begin{aligned} \|p_{k\ell h}^1 + p_{\ell kh}^1\|_{L^2(\Gamma^{k,\ell})} &\leq \|p_{k\ell h}^1 - p_{k,\ell}\|_{L^2(\Gamma^{k,\ell})} + \|p_{\ell kh}^1 - p_{\ell,k}\|_{L^2(\Gamma^{k,\ell})}, \\ \|u_{\ell h}^1 - u_{kh}^1\|_{L^2(\Gamma^{k,\ell})} &\leq \|u_{kh}^1 - u_k\|_{L^2(\Gamma^{k,\ell})} + \|u_{\ell h}^1 - u_\ell\|_{L^2(\Gamma^{k,\ell})}, \end{aligned}$$

so that, using (4.6) and (4.9), we derive for $i = 1, 2$ and $0 \leq m \leq p-1$

$$\|e_i\|_{L^2(\Gamma^{k,\ell})} \leq c\alpha h^{\frac{3}{2}+m} (\|u_k\|_{H^{2+m}(\Omega^k)} + \|u_\ell\|_{H^{2+m}(\Omega^\ell)}) + ch^{\frac{1}{2}+m} \|p_{k,\ell}\|_{H^{\frac{1}{2}+m}(\Gamma^{k,\ell})}. \quad (4.22)$$

Thus, (4.21) yields, for $0 \leq m \leq p-1$,

$$\|\eta_{\ell,k}\|_{L^2(\Gamma^{k,\ell})} \leq ch^{\frac{3}{2}+m} (\|u_k\|_{H^{2+m}(\Omega^k)} + \|u_\ell\|_{H^{2+m}(\Omega^\ell)}) + \frac{ch^{\frac{1}{2}+m}}{\alpha} \|p_{k,\ell}\|_{H^{\frac{1}{2}+m}(\Gamma^{k,\ell})}. \quad (4.23)$$

We can now evaluate $\|\tilde{p}_{k\ell h} - p_{k,\ell}\|_{H^{-\frac{1}{2}}(\Gamma^{k,\ell})}$, using the second equation of (4.13) :

$$\|\tilde{p}_{k\ell h} - p_{k,\ell}\|_{H^{-\frac{1}{2}}(\Gamma^{k,\ell})} \leq \|\epsilon_{k,\ell}\|_{H^{-\frac{1}{2}}(\Gamma^{k,\ell})} + \|p_{k\ell h}^1 - p_{k,\ell}\|_{H^{-\frac{1}{2}}(\Gamma^{k,\ell})}. \quad (4.24)$$

The term $\|p_{k\ell h}^1 - p_{k,\ell}\|_{H^{-\frac{1}{2}}(\Gamma^{k,\ell})}$ is estimated in (4.10), so let us focus on the term $\|\epsilon_{k,\ell}\|_{H^{-\frac{1}{2}}(\Gamma^{k,\ell})}$. From (4.18) we have,

$$\|\epsilon_{k,\ell}\|_{H^{-\frac{1}{2}}(\Gamma^{k,\ell})} \leq \alpha \|\eta_{\ell,k}\|_{H^{-\frac{1}{2}}(\Gamma^{k,\ell})} + \|e_1\|_{H^{-\frac{1}{2}}(\Gamma^{k,\ell})} + \|(Id - \pi_{k,\ell})(\alpha\eta_{\ell,k} + e_1)\|_{H^{-\frac{1}{2}}(\Gamma^{k,\ell})}. \quad (4.25)$$

To evaluate $\|e_1\|_{H^{-\frac{1}{2}}(\Gamma^{k,\ell})}$ we proceed as for $\|e_1\|_{L^2(\Gamma^{k,\ell})}$ and from (4.8) and (4.10) we have, for $i = 1, 2$, for $0 \leq m \leq p-1$,

$$\|e_i\|_{H^{-\frac{1}{2}}(\Gamma^{k,\ell})} \leq c\alpha h^{2+m}(\|u_k\|_{H^{2+m}(\Omega^k)} + \|u_\ell\|_{H^{2+m}(\Omega^\ell)}) + ch^{1+m}\|p_{k,\ell}\|_{H^{\frac{1}{2}+m}(\Gamma^{k,\ell})}.$$

The third term in the right-hand side of (4.25) satisfies

$$\|(Id - \pi_{k,\ell})(\alpha\eta_{\ell,k} + e_1)\|_{H^{-\frac{1}{2}}(\Gamma^{k,\ell})} \leq c\sqrt{h}\|\alpha\eta_{\ell,k} + e_1\|_{L^2(\Gamma^{k,\ell})}.$$

Then, using (4.23) and (4.22) yields, for $0 \leq m \leq p-1$,

$$\begin{aligned} \|(Id - \pi_{k,\ell})(\alpha\eta_{\ell,k} + e_1)\|_{H^{-\frac{1}{2}}(\Gamma^{k,\ell})} &\leq c\alpha h^{2+m}(\|u_k\|_{H^{2+m}(\Omega^k)} + \|u_\ell\|_{H^{2+m}(\Omega^\ell)}) \\ &\quad + ch^{1+m}\|p_{k,\ell}\|_{H^{\frac{1}{2}+m}(\Gamma^{k,\ell})}. \end{aligned}$$

In order to estimate the term $\|\eta_{\ell,k}\|_{H^{-\frac{1}{2}}(\Gamma^{k,\ell})}$ in (4.25), we use (4.19) and then the symmetry of the operator $\pi_{k,\ell}$:

$$2 \int_{\Gamma^{k,\ell}} \eta_{\ell,k} \psi_{\ell,k} = \int_{\Gamma^{k,\ell}} (\psi_{\ell,k} - \pi_{k,\ell}(\psi_{\ell,k})) \eta_{\ell,k} + \frac{1}{\alpha} \int_{\Gamma^{k,\ell}} (e_2 - \pi_{k,\ell}(e_1)) \psi_{\ell,k}.$$

Then, we have

$$\left| \int_{\Gamma^{k,\ell}} \eta_{\ell,k} \psi_{\ell,k} \right| \leq c\sqrt{h}\|\eta_{\ell,k}\|_{L^2(\Gamma^{k,\ell})}\|\psi_{\ell,k}\|_{H^{\frac{1}{2}}(\Gamma^{k,\ell})} + \frac{1}{\alpha}\|e_2 - \pi_{k,\ell}(e_1)\|_{H^{-\frac{1}{2}}(\Gamma^{k,\ell})}\|\psi_{\ell,k}\|_{H^{\frac{1}{2}}(\Gamma^{k,\ell})}$$

from which we deduce that

$$\|\eta_{\ell,k}\|_{H^{-\frac{1}{2}}(\Gamma^{k,\ell})} \leq c\sqrt{h}\|\eta_{\ell,k}\|_{L^2(\Gamma^{k,\ell})} + \frac{c}{\alpha}\|e_2 - \pi_{k,\ell}(e_1)\|_{H^{-\frac{1}{2}}(\Gamma^{k,\ell})}. \quad (4.26)$$

Then, using (4.23) and the fact that

$$\begin{aligned} \|e_2 - \pi_{k,\ell}(e_1)\|_{H^{-\frac{1}{2}}(\Gamma^{k,\ell})} &\leq \|e_2\|_{H^{-\frac{1}{2}}(\Gamma^{k,\ell})} + \|e_1\|_{H^{-\frac{1}{2}}(\Gamma^{k,\ell})} + \|e_1 - \pi_{k,\ell}(e_1)\|_{H^{-\frac{1}{2}}(\Gamma^{k,\ell})} \\ &\leq \|e_2\|_{H^{-\frac{1}{2}}(\Gamma^{k,\ell})} + \|e_1\|_{H^{-\frac{1}{2}}(\Gamma^{k,\ell})} + c\sqrt{h}\|e_1\|_{L^2(\Gamma^{k,\ell})} \end{aligned} \quad (4.27)$$

with (4.22) and (4.26) yields, for $0 \leq m \leq p-1$,

$$\|\eta_{\ell,k}\|_{H^{-\frac{1}{2}}(\Gamma^{k,\ell})} \leq ch^{2+m}(\|u_k\|_{H^{2+m}(\Omega^k)} + \|u_\ell\|_{H^{2+m}(\Omega^\ell)}) + \frac{ch^{1+m}}{\alpha}\|p_{k,\ell}\|_{H^{\frac{1}{2}+m}(\Gamma^{k,\ell})}.$$

Using the previous inequality in (4.25), (4.24) yields, for $0 \leq m \leq p-1$,

$$\|\tilde{p}_{k\ell h} - p_{k,\ell}\|_{H^{-\frac{1}{2}}(\Gamma^{k,\ell})} \leq c\alpha h^{2+m}(\|u_k\|_{H^{2+m}(\Omega^k)} + \|u_\ell\|_{H^{2+m}(\Omega^\ell)}) + ch^{1+m}\|p_{k,\ell}\|_{H^{\frac{1}{2}+m}(\Gamma^{k,\ell})}. \quad (4.28)$$

Let us now estimate $\|\tilde{u}_{\ell h} - u_\ell\|_{H^1(\Omega^\ell)}$:

$$\|\tilde{u}_{\ell h} - u_\ell\|_{H^1(\Omega^\ell)} \leq \|u_{\ell h}^1 - u_\ell\|_{H^1(\Omega^\ell)} + \sum_{k < \ell} \|\mathcal{R}_{\ell,k}(\eta_{\ell,k})\|_{H^1(\Omega^\ell)} \quad (4.29)$$

and from (4.14) and an inverse inequality

$$\|\mathcal{R}_{\ell,k}(\eta_{\ell,k})\|_{H^1(\Omega^\ell)} \leq ch^{-\frac{1}{2}}\|\eta_{\ell,k}\|_{L^2(\Gamma^{k,\ell})}.$$

Hence, from (4.23) we have, for $0 \leq m \leq p-1$,

$$\|\mathcal{R}_{\ell,k}(\eta_{\ell,k})\|_{H^1(\Omega^\ell)} \leq ch^{1+m}(\|u_k\|_{H^{2+m}(\Omega^k)} + \|u_\ell\|_{H^{2+m}(\Omega^\ell)}) + \frac{ch^m}{\alpha} \|p_{k,\ell}\|_{H^{\frac{1}{2}+m}(\Gamma^{k,\ell})},$$

and (4.29) yields, for $0 \leq m \leq p-1$,

$$\begin{aligned} \|\tilde{u}_{\ell h} - u_\ell\|_{H^1(\Omega^\ell)} &\leq ch^{1+m}\|u_\ell\|_{H^{2+m}(\Omega^\ell)} + ch^{1+m} \sum_{k<\ell} \|u_k\|_{H^{2+m}(\Omega^k)} \\ &\quad + \frac{ch^m}{\alpha} \sum_{k<\ell} \|p_{k,\ell}\|_{H^{\frac{1}{2}+m}(\Gamma^{k,\ell})}. \end{aligned} \quad (4.30)$$

which ends the proof of Theorem 3. \square

4.5. Proof of Theorem 4. The proof is the same as for Theorem 3, except that the relation (4.9) for $0 \leq m \leq p-1$ is changed in

$$\|p_{k\ell h}^1 - p_{k,\ell}\|_{L^2(\Gamma^{k,\ell})} \leq ch^{\frac{3}{2}+m} (\log h)^{\beta(m)} \|p_{k,\ell}\|_{H^{\frac{3}{2}+m}(\Gamma^{k,\ell})}. \quad (4.31)$$

The proof of (4.31) is given in Appendix B. Therefore, (4.10) is changed in

$$\|p_{k\ell h}^1 - p_{k,\ell}\|_{H^{-\frac{1}{2}}(\Gamma^{k,\ell})} \leq ch^{2+m} (\log h)^{\beta(m)} \|p_{k,\ell}\|_{H^{\frac{3}{2}+m}(\Gamma^{k,\ell})},$$

the inequalities (4.28) and (4.30) are changed respectively in

$$\begin{aligned} \|\tilde{p}_{k\ell h} - p_{k,\ell}\|_{H^{-\frac{1}{2}}(\Gamma^{k,\ell})} &\leq c\alpha h^{2+m} (\|u_k\|_{H^{2+m}(\Omega^k)} + \|u_\ell\|_{H^{2+m}(\Omega^\ell)}) \\ &\quad + ch^{2+m} (\log h)^{\beta(m)} \|p_{k,\ell}\|_{H^{\frac{3}{2}+m}(\Gamma^{k,\ell})}, \end{aligned}$$

$$\begin{aligned} \|\tilde{u}_{\ell h} - u_\ell\|_{H^1(\Omega^\ell)} &\leq ch^{1+m}\|u_\ell\|_{H^{2+m}(\Omega^\ell)} + ch^{1+m} \sum_{k<\ell} \|u_k\|_{H^{2+m}(\Omega^k)} \\ &\quad + \frac{ch^{1+m}}{\alpha} (\log h)^{\beta(m)} \sum_{k<\ell} \|p_{k,\ell}\|_{H^{\frac{3}{2}+m}(\Gamma^{k,\ell})}. \quad \square \end{aligned}$$

4.6. Error Estimates. Thanks to (3.11), we have the following error estimates:

THEOREM 5. *Assume that the solution u of (2.1)-(2.2) is in $H^2(\Omega) \cap H_0^1(\Omega)$, and $u_k = u|_{\Omega^k} \in H^{2+m}(\Omega^k)$, with $p-1 \geq m \geq 0$, and let $p_{k,\ell} = \frac{\partial u}{\partial \mathbf{n}_k}$ over each $\Gamma^{k,\ell}$. Then, there exists a constant c independent of h and α such that*

$$\begin{aligned} \|\underline{u}_h - \underline{u}\|_* + \|\underline{p}_h - \underline{p}\|_{-\frac{1}{2},*} &\leq c(\alpha h^{2+m} + h^{1+m}) \sum_{k=1}^K \|\underline{u}\|_{H^{2+m}(\Omega^k)} \\ &\quad + c\left(\frac{h^m}{\alpha} + h^{1+m}\right) \sum_{k=1}^K \sum_{\ell} \|p_{k,\ell}\|_{H^{\frac{1}{2}+m}(\Gamma^{k,\ell})}. \end{aligned}$$

THEOREM 6. *Assume that the solution u of (2.1)-(2.2) is in $H^2(\Omega) \cap H_0^1(\Omega)$, $u_k = u|_{\Omega^k} \in H^{2+m}(\Omega^k)$, and $p_{k,\ell} = \frac{\partial u}{\partial \mathbf{n}_k}$ is in $H^{\frac{3}{2}+m}(\Gamma^{k,\ell})$ with $p-1 \geq m \geq 0$. Then there exists a constant c independent of h and α such that*

$$\begin{aligned} \|\underline{u}_h - \underline{u}\|_* + \|\underline{p}_h - \underline{p}\|_{-\frac{1}{2},*} &\leq c(\alpha h^{2+m} + h^{1+m}) \sum_{k=1}^K \|\underline{u}\|_{H^{2+m}(\Omega^k)} \\ &\quad + c\left(\frac{h^{1+m}}{\alpha} + h^{2+m}\right) (\log h)^{\beta(m)} \sum_{k=1}^K \sum_{\ell} \|p_{k,\ell}\|_{H^{\frac{3}{2}+m}(\Gamma^{k,\ell})} \end{aligned}$$

with $\beta(m) = 0$ if $m \leq p-2$ and $\beta(m) = 1$ if $m = p-1$.

5. Numerical results. We consider the initial problem, with exact solution $u(x, y) = x^4 y^4 + xy \cos(10xy)$. The domain is the unit square $\Omega = (0, 1) \times (0, 1)$, decomposed into non-overlapping subdomains with meshes generated independently. In Sections 5.2, 5.3, to observe the numerical error estimates for the discrete problem (2.8), one need to compute the converged solution of the discrete algorithm (3.5)-(3.6) regardless of the algorithm used to compute it. Thus it is the solution at convergence of the algorithm (3.5)-(3.6) with a stopping criterion on the residual (i.e. the jumps of interface conditions) that must be extremely small, e.g. smaller than 10^{-14} . For all the other simulations where we are interested in u_h^n and not u_h , a residual of 10^{-2} times the target H^1 error is considered, for stopping the iterations.

5.1. Choice of the Robin parameter. In our simulations the Robin parameter α is either an arbitrary constant or is obtained by minimizing the convergence factor (depending on the mesh size in that case, see [25]). In the conforming two subdomains case, with constant mesh size h and an interface of length L , the optimal theoretical value of α which minimizes the convergence factor at the continuous level is (see [15]):

$$\alpha_{\text{opt}}(L, h) = [((\frac{\pi}{L})^2 + 1)((\frac{\pi}{h})^2 + 1)]^{\frac{1}{4}}. \quad (5.1)$$

Note that this optimal choice for α does not seem to provide an optimal error estimate from Theorem 5. Nevertheless, as was illustrated in [25] the regularity of the normal derivative of u along the interfaces enters most of the times in the frame of Theorem 6 that allows a larger range of choice for α , compatible with the above mentioned optimal choice (as regards the algorithm).

In the non-conforming case, we consider the following values : $\alpha_{\min} = \alpha_{\text{opt}}(L, \frac{h_{\min}}{p})$, $\alpha_{\text{mean}} = \alpha_{\text{opt}}(L, \frac{h_{\text{mean}}}{p})$, $\alpha_{\max} = \alpha_{\text{opt}}(L, \frac{h_{\max}}{p})$, where h_{\min} , h_{mean} and h_{\max} stands respectively for the smallest, meanest or highest step size on the interface and p is the degree of the approximation.

5.2. H^1 error between the continuous and discrete solutions for \mathbf{P}_2 finite elements. In this part, we compare the relative H^1 error in the non-conforming case to the error obtained on a uniform conforming grid.

We define the relative H^1 error as follows: Let $u_k = u|_{\Omega^k}$, $1 \leq k \leq K$ (where u is the continuous solution), and let $(\underline{u}_h)_k = (\underline{u}_h)|_{\Omega^k}$ where \underline{u}_h is the solution of the discrete problem (2.8). Now, let $N_x = \|u\|_*$ and let $E_k = \|(\underline{u}_h)_k - u_k\|_{H^1(\Omega^k)}$, $1 \leq k \leq K$. Let $E = (\sum_{i=1}^K E_i^2)^{1/2}$. The relative H^1 error is then E/N_x .

We consider four initial meshes : the two uniform conforming meshes (mesh 1 and 4) of Figure 5.1, and the two non-conforming meshes (mesh 2 and 3) of Figure 5.2. In the non-conforming case, the unit square is decomposed into four non-overlapping subdomains numbered as in Figure 5.2 on the left. Figure 5.3 shows the relative H^1 error versus the number of refinement for these four meshes, and $\frac{h^2}{2}$ (where h is the mesh size) versus the number of refinement, in logarithmic scale. At each refinement, the mesh size is divided by two. The results of Figure 5.3 show that the relative H^1 error tends to zero at the same rate as the mesh size squared (h^2), and this fits with the theoretical error estimates of Theorem 6.

On the other hand, we observe that the two curves corresponding to the non-conforming meshes (mesh 2 and mesh 3) are between the curves of the conforming meshes (mesh 1 and mesh 4). We observe that the relative H^1 error for mesh 3 is close to the relative H^1 error for mesh 4 (i.e. the uniform conforming finer mesh), while the one corresponding to mesh 2 is nearly the same as the error for mesh 1 (i.e.

the uniform conforming coarser mesh), as can be expected, as mesh 3 is more refined than mesh 2 in subdomain Ω^4 , where the solution steeply varies.

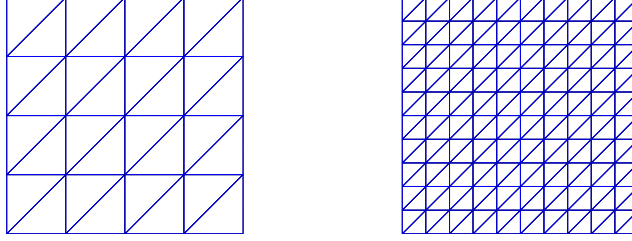


FIG. 5.1. Uniform conforming meshes : mesh 1 (on the left), and mesh 4 (on the right)

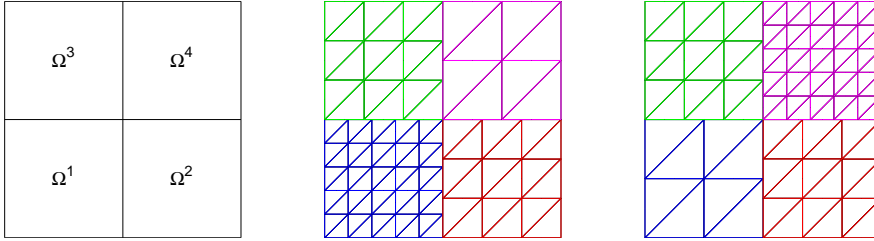


FIG. 5.2. Domain decomposition (on the left), and non-conforming meshes: mesh 2 (on the middle), and mesh 3 (on the right)

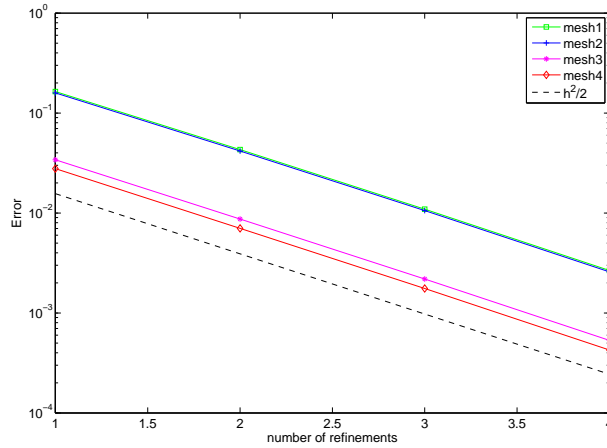


FIG. 5.3. Relative H^1 error versus the number of refinements for the initial meshes : mesh 1, (square line), mesh 2 (plus line), mesh 3 (star line), and mesh 4 (diamond line). The dashed line is $\frac{h^2}{2}$ (where h is the mesh size) versus the number of refinements, in logarithmic scale

5.3. H^1 relative error for different degrees of the finite element approximation. In this part we study the relative H^1 error between the continuous and discrete solutions versus the mesh size, for \mathbf{P}_1 , \mathbf{P}_2 and \mathbf{P}_3 finite elements.

5.3.1. Decomposition into four subdomains. We consider a decomposition of the unit square into four non-overlapping subdomains numbered as in Figure 5.4 on the left. For \mathbf{P}_1 and \mathbf{P}_2 discretizations, we consider the initial non-conforming meshes represented on Figure 5.4 on the middle, and for a \mathbf{P}_3 discretization, we consider the initial non-conforming meshes represented on Figure 5.4 on the right.

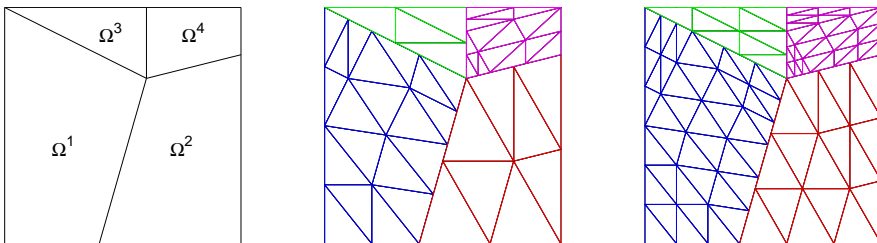


FIG. 5.4. Domain decomposition (left), and non-conforming meshes (middle and right)

Figure 5.5 shows the relative H^1 error between the continuous and discrete solutions versus the mesh size, on the left for \mathbf{P}_1 and \mathbf{P}_2 finite elements, and on the right for \mathbf{P}_3 finite elements, in logarithmic scales. For \mathbf{P}_1 and \mathbf{P}_2 discretizations, we start with the meshes on Figure 5.4 on the middle and divide by 2 the mesh size four times. In order to compute the error, the non-conforming solutions are interpolated on a very fine grid obtained by refining 5 times the initial mesh. For \mathbf{P}_3 discretizations, we start with the meshes on Figure 5.4 on the right and divide by 3 the mesh size three times. In order to compute the error, the non-conforming solutions are interpolated on a very fine grid obtained by refining 4 times the initial meshes.

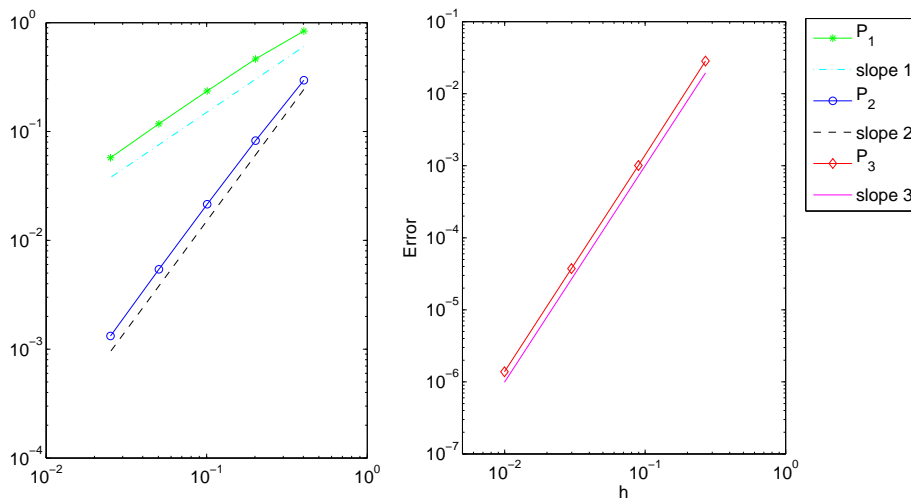


FIG. 5.5. Relative H^1 error versus the mesh size for the non-conforming case. Left: for \mathbf{P}_1 and \mathbf{P}_2 discretizations. Right: for \mathbf{P}_3 discretizations

The results of Figure 5.5 show that if p is the degree of the approximation, the relative H^1 error tends to zero at the same rate as h^p , for $1 \leq p \leq 3$, and this fits with the theoretical error estimates of Theorem 6.

5.3.2. Decomposition into twelve subdomains. We consider the initial problem with exact solution $u(x, y) = x^3y^2 + \sin(xy)$. The domain is $\Omega = (-3, 3) \times (-2, 2)$ and is decomposed into twelve irregularly shaped subdomains as in Figure 5.6. The subdomain meshes are generated in an independent manner as in Figure 5.7. The finite element assemblies are done as in [11].

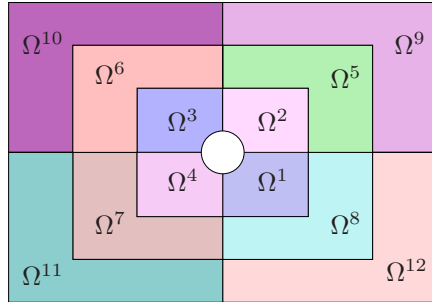


FIG. 5.6. Domain decomposition into twelve non-overlapping subdomains

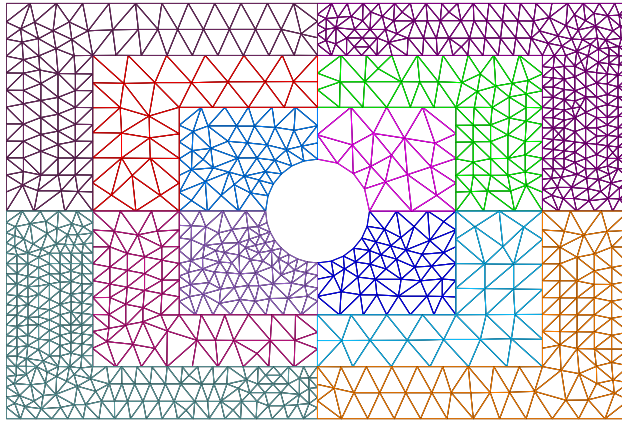


FIG. 5.7. Non-conforming meshes

Figure 5.8 shows the relative H^1 error between the continuous and discrete solutions versus the mesh size, on the left for \mathbf{P}_1 and \mathbf{P}_2 finite elements, and on the right for \mathbf{P}_3 finite elements, in logarithmic scales.

For \mathbf{P}_1 and \mathbf{P}_2 discretizations, we start with the mesh on Figure 5.7 and divide by 2 the mesh size four times. In order to compute the error, the non-conforming solutions are interpolated on a very fine grid obtained by refining 5 times the initial mesh. For \mathbf{P}_3 discretizations, we start with the mesh on Figure 5.7 and divide by 3 the mesh size three times. In order to compute the error, the non-conforming solutions are interpolated on a very fine grid obtained by refining 4 times the initial meshes.

The results of Figure 5.8 show that the relative H^1 error tends to zero at the same rate as h^p , for $1 \leq p \leq 3$ where p is the degree of the approximation. This corresponds to the theoretical error estimates of Theorem 6.

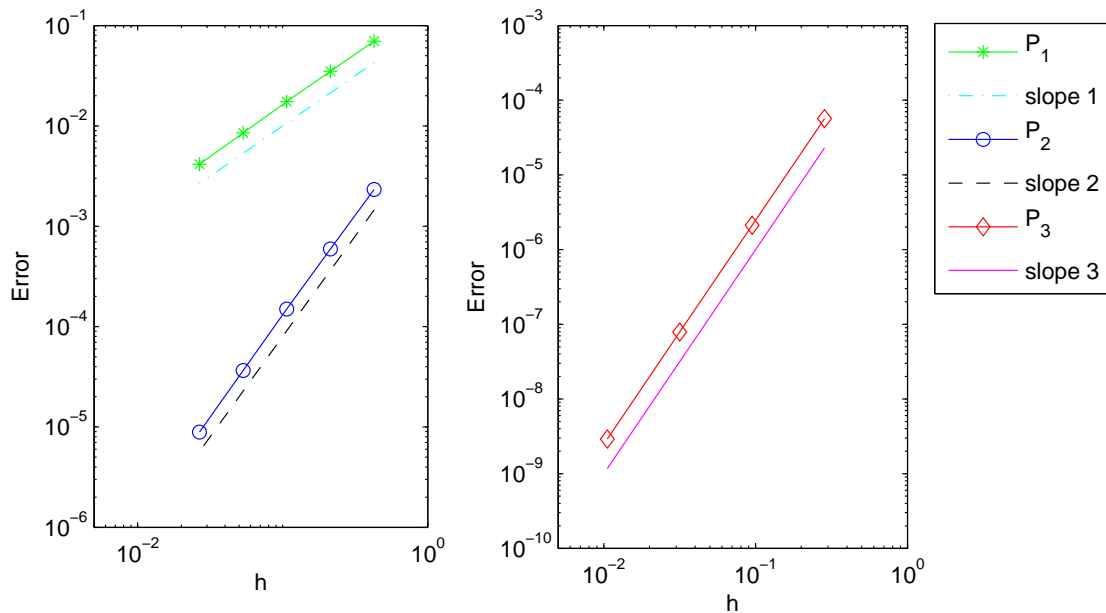


FIG. 5.8. Relative H^1 error versus the mesh size for the non-conforming case. Left: for P_1 and P_2 discretizations. Right: for P_3 discretizations

5.4. Convergence : Choice of the Robin parameter. Let us now study the convergence speed to reach the discrete solution, for different values of the Robin parameter α , in the case of P_2 finite elements. We first consider a domain decomposition in two subdomains, and then in four subdomains as shown in Figure 5.9. We simulate the error equations (i.e. $f = 0$), and use a random initial guess so that all the frequency components are present.

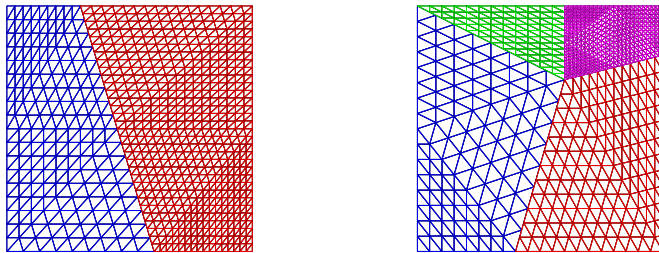


FIG. 5.9. Domain decomposition in two subdomains (left) and in four subdomains (right), with non-conforming meshes

5.4.1. 2 subdomain case. In this part, the unit square is decomposed into two subdomains with non-conforming meshes (with 703 and 2145 nodes respectively) as shown in Figure 5.9 (on the left).

On Figure 5.10 (top left) we represent the H^1 norm of the iterate error, for different values of the Robin parameter α . We observe that the optimal numerical value of the Robin parameter is close to α_{\min} . As the relative H^1 error didn't show where the error is highest, we also represented on Figure 5.10 (top right) the L^∞ norm of the iterate error, for different values of the Robin parameter α . We obtain similar results as for the relative H^1 error.

The Schwarz algorithm can be interpreted as a Jacobi algorithm applied to an interface problem (see [33]). In order to accelerate the convergence, we can replace the Jacobi algorithm by a GMRES ([34]) algorithm. Figure 5.10 show respectively the H^1 norm (on the bottom left) and the L^∞ norm (on the bottom right) of the GMRES iterate error, for different values of the Robin parameter α .

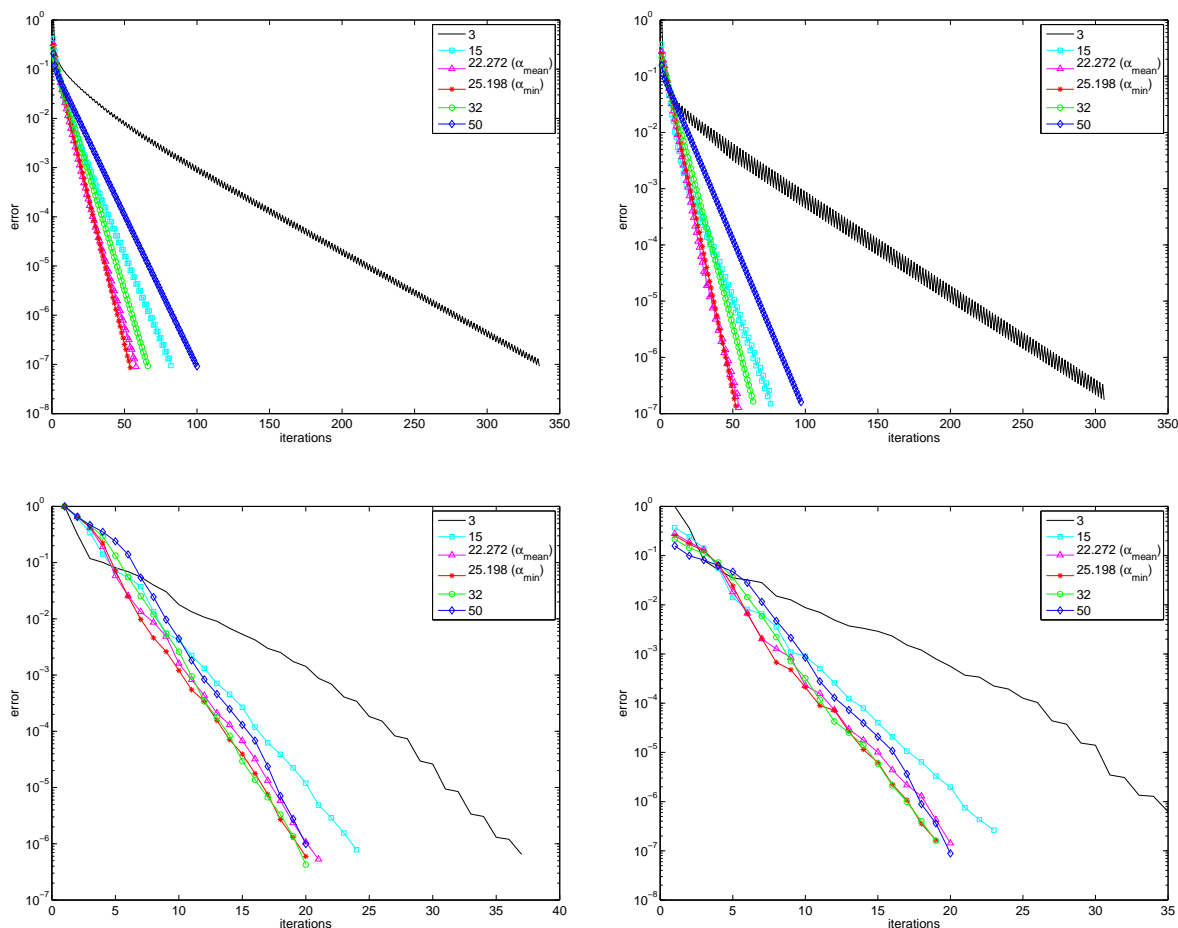


FIG. 5.10. Error versus Schwarz (top) or Gmres (bottom) iterations for different values of the Robin parameter α . Left: the H^1 error, right: the L^∞ error.

For $\alpha = \alpha_{\min}$, the convergence is accelerated by a factor 2 for GMRES, compared to the Schwarz algorithm. Moreover, the gap between the error values for different α is decreasing when using the GMRES algorithm, compared to the Schwarz method. Thus, the GMRES algorithm is less sensitive to the choice of the Robin parameter.

The sensitivity of the performance of the Krylov solver to the optimized value of the parameter is thus not so critical but it is real and especially visible for ranges of accuracy used for most practical applications (relative errors of size 10^{-2} or 10^{-3}). Adding that this effect generally increases with the number of subdomains and the refinement of the mesh [15] together with the complexity of the equations, we advise when possible to look for the optimized value. Moreover, this conclusion on the interest of GMRES compared to Schwarz is established for stationary problems but is not yet verified for time dependent problems with a Schwarz waveform relaxation algorithm, as illustrated for example in [21].

In Table 5.1 we show the number of iterations N to reduce the H^1 error by a factor 10^6 versus the Robin parameter α , for different degrees p of the approximation. We observe that α_{\min} is very close to the optimal numerical value, for all $p = 1, 2, 3$.

α	N ($p = 1$)	α	N ($p = 2$)	α	N ($p = 3$)
10	57	17	63	23	88
15	40	22	51	28	74
17.818 (α_{\min})	36	25.198 (α_{\min})	49	30.861 (α_{\min})	68
20	39	27	52	33	66
25	40	32	61	35	68
30	58	37	71	40	77

TABLE 5.1

Number of iterations to reduce the H^1 error by a factor 10^6 versus α , for different degrees p

5.4.2. 4 subdomain case. In this part, the unit square is decomposed into four subdomains with non-conforming meshes as shown in Figure 5.9 (on the right).

From the results of Section 5.4.1, we will consider for the optimized parameter α the values given by the smallest mesh size on the interface. As we have four interfaces, using formula (5.1) with $h = h_{\min}^{k,\ell}$, $1 \leq k, \ell \leq 4$, with $\Gamma^{k,\ell}$ not empty, we obtain four values given by: $\alpha_{\min}^{1,2} = 18.479$, $\alpha_{\min}^{1,3} = 19.250$, $\alpha_{\min}^{2,4} = 34.725$, $\alpha_{\min}^{3,4} = 40.709$. We define α^* the parameter with these four values over the interfaces (i.e. α^* is constant over each interface, with different constants from one interface to another). We consider also a constant optimized value α_{\min} over the four interfaces obtained by taking $h = \min(h_{\min}^{1,2}, h_{\min}^{1,3}, h_{\min}^{2,4}, h_{\min}^{3,4})$ in formula (5.1). We obtain $\alpha_{\min} = \alpha_{\min}^{3,4} = 40.709$. On Figure 6.1 we represent the H^1 norm of the error, for α^* , α_{\min} and for different constant values of the Robin parameter α , with the Schwarz method on the left, and the GMRES algorithm on the right.

We observe that the optimal numerical value of the Robin parameter is close to α_{\min} . We also observe in that case that taking the different optimized values over the interfaces (i.e. α^*) doesn't improve substantially the convergence speed compared to taking the same value α_{\min} over the interfaces.

6. Conclusions. We have analyzed the convergence of the iterative algorithm for \mathbf{P}_p finite elements, with $p \geq 1$ in 2D and $p = 1$ in 3D, for the NICEM method. It relies on Schwarz type algorithms with Robin interface conditions on non-conforming grids. We have extended the error estimates in 2D for piecewise polynomials of higher order. Numerical results show that the method preserves the order of the finite elements for \mathbf{P}_p discretizations, with $p = 1, 2$ or 3 .

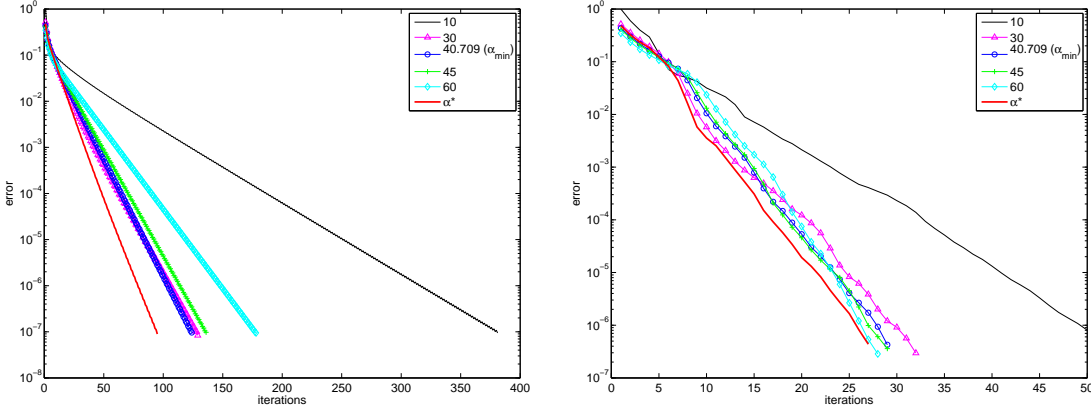


FIG. 6.1. Error versus iterations, for different values of the Robin parameter α . Left: the Schwarz algorithm, right: the GMRES algorithm.

Appendix A. Proof of Lemma 6 in the case $p \geq 3$. From Section 4.2, it remains to prove Lemma 6 in the general case $p \geq 3$. Let us introduce the vector space $Q^p = \{\eta \in \mathbf{P}_p([-1, 1]) \text{ s.t. } \eta(-1) = 0\}$. The function $\Delta(\eta)$ is quadratic so that it suffices to study the extrema of $\Delta(\eta)/\|\eta\|_{L^2([-1, 1])}^2$ over Q^p or equivalently to prove that the associated symmetric quadratic form is negative, i.e. its eigenvalues are negative. They correspond to the Lagrange multiplier solutions μ_1 of the following min-max problem

$$\min_{\eta \in Q^p} \max_{\mu_1 \in \mathbb{R}} \mathcal{L}_e(\eta, \mu_1), \quad (\text{A.1})$$

where

$$\mathcal{L}_e(\eta, \mu_1) := \Delta(\eta) - \mu_1(\|\eta\|_{L^2([-1, 1])}^2 - 1).$$

We have to prove that $\mu_1 < 0$. We have

$$\begin{aligned} 0 &= \left\langle \frac{\partial \mathcal{L}_e}{\partial \eta}, \delta \eta \right\rangle \\ &= 2(2\eta(1) - 3\eta_p)(2\delta\eta(1) - 3\delta\eta_p) + p^2(-8 \langle \eta, \delta \eta \rangle + 18 \frac{\eta_p \delta \eta_p}{2p+1}) - 2\mu_1 \langle \eta, \delta \eta \rangle \end{aligned}$$

where $\langle \cdot, \cdot \rangle$ denotes the L^2 scalar product on $L^2([-1, 1])$ and $\delta \eta \in Q^p$.

Let us consider the vector space $(1-x^2)\mathbf{P}_{p-3} \subset Q^p$. Any function γ in $(1-x^2)\mathbf{P}_{p-3}$ satisfies $\gamma(-1) = \gamma(1) = 0$ and $\gamma_p = 0$. The optimality relation w.r.t. to $(1-x^2)\mathbf{P}_{p-3}$ gives

$$(-8p^2 - 2\mu_1) \langle \eta, \delta \eta \rangle = 0, \quad \forall \delta \eta \in (1-x^2)\mathbf{P}_{p-3}.$$

We have either $\mu_1 = -4p^2 < 0$ or η solution to (A.1) belongs to the space $\{(1-x^2)\mathbf{P}_{p-3}\}^\perp \cap \mathbf{P}_p$. The first case corresponds to a negative value for μ_1 which is in agreement with the lemma to be proved. Let us study the latter case. We shall make use of (see [3])

LEMMA 7. *The family of Legendre polynomials satisfies*

$$\begin{aligned} \int_{-1}^1 L'_m L'_{m'} (1-x^2) dx &= 0, \quad m \neq m', \\ \int_{-1}^1 L'_m{}^2 &= m(m+1), \\ \int_{-1}^1 L'_m L'_{m+1} &= 0, \\ \int_{-1}^1 L'_{m-1} L'_{m+1} &= m(m-1), \\ L'_m(-1) &= (-1)^{m+1} \frac{m(m+1)}{2}. \end{aligned}$$

For any p , $p \geq 3$,

$$\{(1-x^2)\mathbf{P}_{p-3}\}^\perp \cap \mathbf{P}_p = \text{Span}\{L_p, L'_p, L'_{p-1}\}.$$

Proof. We only need to prove the last equality, that results from the above indeed it can be checked easily that

$$\{(1-x^2)\mathbf{P}_{p-3}\}^\perp \cap \mathbf{P}_p = \text{Span}\{L'_{p+1}, L'_p, L'_{p-1}\}.$$

Moreover, we have

$$L'_{p+1}(x) = (2p+1)L_p(x) + L'_{p-1}(x)$$

and thus Lemma 7.

Therefore, there exists $\lambda_1, \lambda_2, \lambda_3 \in \mathbb{R}$ s.t. $\eta = \lambda_1 L_p + \lambda_2 L'_p + \lambda_3 L'_{p-1}$. Since η is defined up to a constant, we only have to consider the two cases $\lambda_1 = 1$ or $\lambda_1 = 0$.

Case 1: $\lambda_1 = 1$

From $\eta(-1) = 0$, we get

$$1 - \lambda_2 \frac{p(p+1)}{2} + \lambda_3 \frac{p(p-1)}{2} = 0,$$

so that

$$\lambda_2 = \frac{2}{p(p+1)} + \lambda_3 \frac{p-1}{p+1},$$

$$\Delta(\eta) = -4 \frac{(p-1)p^2(p^2+1)}{p+1} \lambda_3^2 - \frac{(24p^4 - 20p^3 - 8p^2 + 4p)}{(p+1)(2p+1)} \lambda_3 - \frac{29p^2 + 13p - 1 - p^3}{(p+1)(2p+1)}.$$

Since p is supposed larger than 1, the leading coefficient of $\Delta(\eta)$ is negative. If the discriminant of $\Delta(\eta)$ is negative, the polynomial is negative for any λ_3 . This discriminant has the value

$$16 \frac{(p^2 - 13p - 8)(p-1)p^3}{2p+1}$$

and is negative for $2 \leq p \leq 13$.

Case 2: $\lambda_1 = 0$

From $\eta(-1) = 0$, we get

$$-\lambda_2 \frac{p(p+1)}{2} + \lambda_3 \frac{p(p-1)}{2} = 0,$$

so that

$$\lambda_2 = \lambda_3 \frac{p-1}{p+1}.$$

Since η is an eigenvalue, it is not zero and the above relation shows that we can take $\lambda_3 = 1$. Then, we have $\lambda_2 = \frac{p-1}{p+1}$ so that

$$\Delta(\eta) = \frac{-4(p-1)p^2(p^2+1)}{(p+1)} < 0,$$

which ends the proof of Lemma 6. \square

Appendix B. Proof of the estimate (4.31). For $0 \leq m < p-1$, $\beta(m) = 0$ and the estimate (4.31) is standard. For $m = p-1$, the proof is the same as for Lemma 5 in [25]: let $\bar{p}_{k\ell h}$ be the unique element of $\tilde{W}_h^{k,\ell}$ defined as follows :

- $(\bar{p}_{k\ell h})|_{[x_1^{\ell,k}, x_{N-1}^{\ell,k}]}$ coincide with the interpolate of degree p of $p_{k,\ell}$.
- $(\bar{p}_{k\ell h})|_{[x_0^{\ell,k}, x_1^{\ell,k}]}$ and $(\bar{p}_{k\ell h})|_{[x_{N-1}^{\ell,k}, x_N^{\ell,k}]}$ coincide with the interpolate of degree $p-1$ of $p_{k,\ell}$.

Then, using Deny-Lions theorem we have

$$\begin{aligned} \|p_{k\ell h}^1 - p_{k,\ell}\|_{L^2(\Gamma^{k,\ell})}^2 &\leq \|\bar{p}_{k\ell h} - p_{k,\ell}\|_{L^2([x_0^{\ell,k}, x_1^{\ell,k}])}^2 \\ &\quad + ch^{1+2p} \|p_{k,\ell}\|_{H^{\frac{1}{2}+p}([x_1^{\ell,k}, x_{N-1}^{\ell,k}])}^2 + \|\bar{p}_{k\ell h} - p_{k,\ell}\|_{L^2([x_{N-1}^{\ell,k}, x_N^{\ell,k}])}^2. \end{aligned}$$

In order to analyze the two extreme contributions, we use Deny-Lions theorem

$$\|\bar{p}_{k\ell h} - p_{k,\ell}\|_{L^2([x_0^{\ell,k}, x_1^{\ell,k}])}^2 \leq ch^{1+2p-\frac{2}{q}} \left\| \frac{d^p p_{k,\ell}}{dx^p} \right\|_{L^q([x_0^{\ell,k}, x_1^{\ell,k}])}^2,$$

and taking $q = -\log(h)$, we finish the proof as for Lemma 5 in [25]. \square

Acknowledgment. The authors would like to thank François Cuvelier for his help in the implementation of the test case of Section 5.3.2, especially for his development of a FreeFem++ code that generates automatically the meshes with different refinement levels, that we used for our numerical results.

REFERENCES

- [1] Y. ACHDOU, C. JAPHET, Y. MADAY AND F. NATAF, *A new cement to glue non-conforming grids with Robin interface conditions: the finite volume case*, Numer. Math., 92 (2002), No. 4, pp. 593-620.
- [2] Y. ACHDOU, Y. MADAY AND O. WIDLUND, *Iterative Substructuring Preconditioners for Mortar Element Methods in Two Dimensions*, SIAM J. Numer. Anal., 2 (1999), pp. 551-580.
- [3] M. ABRAMOWITZ AND I. A. STEGUN, *Handbook of mathematical functions with formulas, graphs, and mathematical tables*, Dover Publications Inc., New York (1992), Reprint of the 1972 edition
- [4] J.D. BENAMOU AND B. DESPRÈS, *A Domain Decomposition Method for the Helmholtz equation and related Optimal Control Problems*, J. Comp. Phys., 136 (1997) pp. 68-82.

- [5] F. BEN BELGACEM, *The Mortar finite Element Method with Lagrange Multipliers*, Numer. Math., 84(2) (1999), pp. 173-197.
- [6] F. BEN BELGACEM AND Y. MADAY, *Coupling spectral and finite elements for second order elliptic three-dimensional equations*, SIAM J. Numer. Anal., 36 (1999), No. 4, pp. 1234-1263.
- [7] C. BERNARDI AND V. GIRAULT, *A local regularization operator for triangular and quadrilateral finite elements*, SIAM J. Numer. Anal., 35 (1998), No. 5, pp. 1893-1916. Kiel (1986).
- [8] C. BERNARDI, Y. MADAY AND A. PATERA, *A new nonconforming approach to domain decomposition: the mortar element method*, Nonlinear Partial Differential Equations and their Applications, eds H. Brezis and J.L. Lions, Pitman (1989).
- [9] D. BRAESS AND W. DAHMEN, *Stability estimates of the mortar finite element method for 3-dimensional problems*, East-West J. Numer. Math., 6 (1998), No. 4, pp. 249-263.
- [10] A. DE LA BOURDONNAYE, C. FAHRAT, A. MACEDO, F. MAGOULÈS AND F.X. ROUX, *A Nonoverlapping Domain Decomposition Method for the Exterior Helmholtz Problem*, DD10 Proceedings, (1997).
- [11] F. CUVELIER, C. JAPHET AND G. SCARELLA, *An efficient way to perform the assembly of finite element matrices in Matlab and Octave*, Preprint, Université Paris 13 and INRIA, <http://hal.inria.fr/hal-00821942>, 2013.
- [12] B. DESPRÈS, *Domain decomposition method and the Helmholtz problem*, Mathematical and Numerical aspects of wave propagation phenomena, SIAM, (1991) pp. 44-52.
- [13] B. DESPRÈS, *Domain decomposition method and the Helmholtz problem. II*, Kleinman Ralph (eds) et al., Mathematical and numerical aspects of wave propagation. Proceedings of the 2nd international conference held in Newark, DE, USA, June 7-10, 1993. Philadelphia, PA: SIAM, (1993), pp. 197-206.
- [14] B. DESPRES, P. JOLY AND J. E. ROBERTS, International Symposium on Iterative methods in linear algebra, Brussels, Belgium, (1991), pp. 475-484.
- [15] M. J. GANDER, *Optimized Schwarz Methods*, SIAM Journal on Numerical Analysis, Vol. 44, No. 2, pp. 699-731, 2006.
- [16] M. J. GANDER, C. JAPHET, Y. MADAY, F. NATAF, *A new cement to glue non-conforming grids with Robin interface conditions: the finite element case*, Domain Decomposition Methods in Science and Engineering Series : Lecture Notes in Computational Science and Engineering, Vol. 40, Kornhuber, R.; Hoppe, R.; Periaux, J.; Pironneau, O.; Widlund, O.; Xu, J. (Eds.), (2004).
- [17] F. GASTALDI, L. GASTALDI AND A. QUARTERONI, *Adaptative Domain Decomposition Methods for Advection dominated Equations*, East-West J. Numer. Math., 4 (1996), pp. 165-206.
- [18] S. GHANEMI, *Méthode de décomposition de domaines avec conditions de transmissions non locales pour des problèmes de propagation d'ondes*, PhD thesis, Université Paris IX Dauphine (1996).
- [19] S. GHANEMI, P. JOLY AND F. COLLINO, *Domain decomposition method for harmonic wave equations*, Third international conference on mathematical and numerical aspect of wave propagation, (1995), pp. 663-672.
- [20] T. HAGSTROM, R. P. TEWARSON AND A. JAZCILEVICH, *Numerical Experiments on a Domain Decomposition Algorithm for Nonlinear Elliptic Boundary Value Problems*, Appl. Math. Lett., 1 (1988), No. 3, pp. 299-302.
- [21] T.T.P. HOANG, J. JAFFRÉ, C. JAPHET, M. KERN AND J. ROBERTS. *Space-time domain decomposition methods for diffusion problems in mixed formulation*, accepted SIAM J. Num. Anal, 2013.
- [22] C. JAPHET, *Méthode de décomposition de domaine et conditions aux limites artificielles en mécanique des fluides: méthode Optimisée d'Ordre 2 (OO2)*, PhD thesis, Université Paris 13 (1998).
- [23] C. JAPHET, *Optimized Krylov-Ventcell Method. Application to Convection-Diffusion Problems*, Proceedings of the 9th International Conference on Domain Decomposition Methods, 3-8 june 1996, Bergen (Norway), Domain Decomposition Methods in Sciences and Engineering, edited by P. Bjorstad, M. Espedal and D. Keyes (1998), p. 382-389.
- [24] C. JAPHET, F. NATAF AND F. ROGIER, *The Optimized Order 2 Method. Application to convection-diffusion problems*, Future Generation Computer Systems, 18(1) (2001), pp. 17-30, Elsevier Science.
- [25] C. JAPHET, Y. MADAY, F. NATAF, *A New Interface Cement Equilibrated Mortar (NICEM) Method With Robin Interface Conditions: the \mathbf{P}_1 finite element case*, M3AS, Volume No.23, Issue No. 12., 2013.
- [26] C. JAPHET, Y. MADAY, F. NATAF, *NICEM method with Ventcel conditions*, Proceedings of the 21th International Conference on Domain Decomposition Methods, Rennes (France), 2013.

- [27] C. LACOUR, *Analyse et Résolution Numérique de Méthodes de Sous-Domains Non Conformés pour des Problèmes de Plaques*, PhD thesis, Université Pierre et Marie Curie (1997).
- [28] S. C. LEE, M. N. VOUVAKIS AND J. F. LEE, *A non-overlapping domain decomposition method with non-matching grids for modeling large finite antenna arrays*, J. Comput. Phys., 203 (1) (2005), pp. 1-21.
- [29] B. LICHTENBERG, B. WEBB, D. MEADE AND A. F. PETERSON, *Comparison of two-dimensional conformal local radiation boundary conditions*, Electromagnetics 16, (1996), pp. 359-384.
- [30] P.L. LIONS, *On the Schwarz Alternating Method III: A Variant for Nonoverlapping Subdomains*, Third International Symposium on Domain Decomposition Methods for Partial Differential Equations, SIAM (1989), pp. 202-223.
- [31] L.C. MCINNES, R.F. SUSAN-RESIGA, D. E. KEYES AND H. M. ATASSI, *Additive Schwarz methods with nonreflecting boundary conditions for the parallel computation of Helmholtz problems*, in Xiao-Chuan Cai, Charbel Farhat and Jan Mandel, editors, Tenth International Symposium on Domain Decomposition Methods for Partial Differential Equations, AMS, (1997).
- [32] F. NATAF AND F. ROGIER, *Factorization of the Convection-Diffusion Operator and the Schwarz Algorithm*, M³AS, 5 (1995), No. 1, pp. 67-93.
- [33] F. NATAF, F. ROGIER AND E. DE STURLER, *Domain Decomposition Methods for Fluid Dynamics, Navier-Stokes Equations and Related Nonlinear Analysis*, Edited by A. Sequeira, Plenum Press Corporation, (1995), pp. 367-376.
- [34] Y. SAAD, *Iterative Methods for Sparse Linear Systems*, SIAM eds., 2003.
- [35] L. SAAS, I. FAILLE, F. NATAF AND F. WILLIEN, *Finite Volume Methods for Domain Decomposition on Nonmatching Grids with Arbitrary Interface Conditions*, SIAM J. Num. Ana., 43 (2005), No. 2, pp. 860-890.
- [36] A. TOSELLI AND O. WIDLUND, *Domain decomposition methods—algorithms and theory*, Springer Series in Computational Mathematics, 34 (2005), Springer-Verlag.
- [37] P. E. J. VOS, S. SPENCER AND R. M. KIRBY *From h to p efficiently: Implementing finite and spectral/hp element methods to achieve optimal performance for low- and high-order discretisations*, Journal of Computational Physics, 229 -13, pp 5161-5181, (2010).
- [38] O.B. WIDLUND, *An extension theorem for finite element spaces with three applications*, Numerical Techniques in Continuum Mechanics, Proc. Second GAMM Seminar, Kiel (1986).